Available online at www.sciencedirect.com
ScienceDirect
European Journal of Mechanics B/Fluids 27 (2008) 444–465

Database for flows of binary gas mixtures through a plane microchannel

Shingo Kosuge [a,*,1], Shigeru Takata [b]

[a] *Laboratoire MIP, Université Paul Sabatier, 118 route de Narbonne, 31062 Toulouse Cedex 4, France*
[b] *Department of Mechanical Engineering and Science and Advanced Research Institute of Fluid Science and Engineering, Graduate School of Engineering, Kyoto University, Kyoto 606-8501, Japan*

Received 7 December 2006; received in revised form 26 July 2007; accepted 12 August 2007

Available online 19 August 2007

Abstract

A binary mixture of rarefied gases between two parallel plates is considered. The Poiseuille flow, thermal transpiration (flow caused by a temperature gradient of the plates) and concentration-driven flow (flow caused by a gradient of concentration of the component species) are analyzed on the basis of the linearized model Boltzmann equation with the diffuse reflection boundary condition. The analyses are first performed for mixtures of virtual gases composed of the hard-sphere or Maxwell molecules and the results are compared with those of the original Boltzmann equation. Then, the analyses for noble gases (He–Ne, He–Ar and Ne–Ar) are performed assuming more realistic molecular models (the inverse power-law potential and Lennard-Jones 12,6 models). By use of the results, flux databases covering the entire ranges of the Knudsen number and of the concentration and a wide range of the temperature are constructed. The databases are prepared for the use in the fluid-dynamic model for mixtures in a stationary nonisothermal microchannel derived in [S. Takata, H. Sugimoto, S. Kosuge, Eur. J. Mech. B/Fluids 26 (2007) 155], but can also be incorporated in the generalized Reynolds equation [S. Fukui, R. Kaneko, J. Tribol. 110 (1988) 253] in the gas film lubrication theory. The databases constructed can be downloaded freely from Electronic Annex 2 in the online version of this article.

PACS: 51.10.+y; 05.20.Dd; 47.45.-n; 47.60.+i; 47.70.Nd

Keywords: Boltzmann equation; Kinetic theory of gases; Binary mixture; Poiseuille flow; Thermal transpiration; Concentration-driven flow; Channel flow

1. Introduction

A precise description of gas flows through a microchannel becomes practically important in connection with the recent development of the micro-electro-mechanical systems (MEMS) engineering. As the width of the microchannel becomes comparable to the molecular mean free path, the behaviour of gas in the channel should be described not

* Corresponding author.
E-mail address: kosuge@aero.mbox.media.kyoto-u.ac.jp (S. Kosuge).
[1] Permanent address: Department of Mechanical Engineering and Science and Advanced Research Institute of Fluid Science and Engineering, Graduate School of Engineering, Kyoto University, Kyoto 606-8501, Japan.

0997-7546/$ – see front matter
doi:10.1016/j.euromechflu.2007.08.002

by the conventional fluid dynamics but by the rarefied gas dynamics, and one usually must resort to time-consuming computations of the Boltzmann system. In the case of low Mach number flows through a very long channel (more precisely, the characteristic length of the variation of physical state along the channel is much larger than its width), however, one may save the computational resource by the use of the fluid-dynamic models, even when the Knudsen number [= (mean free path)/(channel width)] is not small. A well-known example is the generalized Reynolds equation, which was proposed in Ref. [1] for the gas film lubrication problem and was recently applied also to the microchannel flow problem in Ref. [2] (the degenerated Reynolds equation). Similar fluid-dynamic model for a binary gas mixture in a stationary nonisothermal microchannel was devised recently in Ref. [3] to investigate the effect of the gas separation induced by the Knudsen compressor [4–6].

Those fluid-dynamic models describe the mass conservation at each cross section of the channel, making use of data of the mass flux obtained in the analyses of the elemental channel-flow problems based on the linearized Boltzmann equation (see, e.g., Refs. [2,7]). In the case of the model devised in Ref. [3], for example, those elemental flows are the Poiseuille flow, thermal transpiration (flow caused by a temperature gradient of the channel wall; see, e.g., Refs. [8,9]) and *concentration-driven flow* (flow caused by a gradient of concentration of the component species of the mixture) between two parallel plates. Before starting analyses by the use of the fluid-dynamic model in Ref. [3], therefore, one needs to prepare the flux data of those flows for local values of the Knudsen number, concentration and temperature at every cross section and at every moment. The purpose of the present contribution is to construct and to provide the flux database of the above three elemental flows which covers the entire ranges of the Knudsen number and of the concentration and a wide range of the temperature. Such a database can readily be incorporated in the fluid-dynamic model in Ref. [3] and also in the generalized Reynolds equation for binary mixtures.

The elemental channel-flows mentioned above have been intensively studied on the basis of the linearized Boltzmann equation mainly in the case of single-component gases (see, e.g., Refs. [10,11] and references therein), while the study of such flows began focusing on the case of gas mixtures (e.g., Refs. [12–19]), because of the increasing demand for their detailed information in practical situations. Indeed, the Poiseuille flow, thermal transpiration and concentration-driven flow of binary gas mixtures through a plane channel have already been analyzed on the basis of the linearized Boltzmann equation in Ref. [19] and its model equation proposed by F.J. McCormack [20] in Refs. [12, 16,17]. As a result, the behaviour of macroscopic quantities and the velocity distribution function of gas molecules as well as the fluxes for a wide range of parameters were obtained in detail. In the present work, we will again analyze the above three elemental flows of gas mixtures on the basis of McCormack's model as in Refs. [12,16,17], but we stress here that our main purpose is to construct and to provide their flux database that covers the entire range of both the Knudsen number and the concentration. The database must also cover a wide range of temperature. To this end, we use four different approaches depending on the Knudsen number regimes in the construction, i.e., the asymptotic analysis for small Knudsen numbers (typically the Knudsen number $\mathrm{Kn} \lesssim 0.01$), the direct numerical solution by a finite-difference method ($0.01 \lesssim \mathrm{Kn} \lesssim 400$), the conversion to a system of integral equations and its direct numerical solution ($100 \lesssim \mathrm{Kn} \lesssim 10^6$), and the analytical asymptotic solution for $\mathrm{Kn} \to \infty$. The reason for this combination will be clear subsequently. In each regime, the numerical computation is carried out for discrete values of the Knudsen number, concentration and temperature. The flux database is then constructed by the Chebyshev polynomial interpolation with respect to the former two and by the spline interpolation with respect to the latter. The database thus constructed is provided as Electronic Annex 2 in the online version of this article.

The paper is organized as follows. To begin with, we formulate the problem in Section 2 on the basis of the McCormack model equation and present the boundary-value problem to be solved. This problem is directly and numerically solved for intermediate Knudsen numbers. In Section 3, we first carry out the asymptotic analysis of the problem for small Knudsen numbers and derive the half-space problem (the Knudsen-layer problem) to be solved numerically (Section 3.1). Then, we transform the boundary-value problem in Section 2 to a system of integral equations for macroscopic quantities, which is used for the analysis for large Knudsen numbers (Section 3.2). This transformation is possible because we adopt the model equation in place of the original Boltzmann equation. The resulting system is solved numerically for large Knudsen numbers. It is also used to obtain the asymptotic behaviour of the mixtures when $\mathrm{Kn} \to \infty$. The method of flux database construction from the results of the analyses is given in Section 4. The database is prepared for the following two kinds of mixture: (i) mixtures of virtual gases composed of the hard-sphere (HS) or Maxwell molecules and (ii) mixtures of noble gases, i.e., He–Ne, He–Ar and Ne–Ar. In the latter case, we assume the HS, Maxwell, inverse-power-law (IPL) potential and Lennard-Jones (LJ) 12,6 molecular models. Finally, after a brief summary of the data of computation in Section 5, we conclude the paper in Section 6.

2. Formulation of the problem

2.1. Problem and assumption

Consider a binary mixture of rarefied gases, say species A and B, between two parallel plates at rest. One of the plates is located at $X_2 = D/2$ and the other at $X_2 = -D/2$, where X_i is the rectangular coordinate system. Both of the plates are kept at common temperature $T_0(1 + C_T X_1/D)$ with C_T and T_0 being constants, i.e., there is a uniform temperature gradient in the X_1-direction. The pressure p of the mixture and the concentration χ^A (the molecular number fraction) of species A have also uniform gradients in the X_1-direction and are given by $p_0(1 + C_P X_1/D)$ and $\chi_0^A + C_\chi X_1/D$ respectively, where C_P, C_χ, p_0 and χ_0^A are constants (one can seek a solution whose pressure and concentration are independent of X_2 in the linear analysis; see the sentence below and Section 2.2). On the assumption that the (nondimensional) gradients C_P, C_T and C_χ are small, we investigate the steady flow of the mixture on the basis of the McCormack model [20] for the linearized Boltzmann equation with the diffuse reflection boundary condition. Note that the concentration $\chi^B (= 1 - \chi^A)$ of species B is given by $\chi_0^B - C_\chi X_1/D$ ($\chi_0^B = 1 - \chi_0^A$) by definition, i.e., the gradient of χ^B has the same magnitude as that of χ^A but the direction is opposite.

Let us now summarize the main notation used in the paper. In the sequel, the Greek letters α and β will be used symbolically to represent the gas species, i.e., $\{\alpha, \beta\} = \{A, B\}$. The n_0 is the reference molecular number density of the mixture and is defined by $n_0 = p_0/\kappa T_0$, where κ is the Boltzmann constant. The x_i is the nondimensional coordinate system defined by $x_i = X_i/D$. The m^α is the molecular mass of species α, $(2\kappa T_0/m^A)^{1/2}\zeta_i$ [or $(2\kappa T_0/m^A)^{1/2}\boldsymbol{\zeta}$] the molecular velocity and $n_0(m^A/2\kappa T_0)^{3/2}(\chi_0^\alpha + \phi^\alpha)E^\alpha$ the velocity distribution function of the molecules of species α, where $E^\alpha(\boldsymbol{\zeta}) = (\hat{m}^\alpha/\pi)^{3/2}\exp(-\hat{m}^\alpha|\boldsymbol{\zeta}|^2)$ with $\hat{m}^\alpha = m^\alpha/m^A$. The molecular number density, flow velocity, pressure, temperature, stress tensor and heat-flow vector of species α are denoted, respectively, by $n_0(\chi_0^\alpha + \omega^\alpha)$, $(2\kappa T_0/m^A)^{1/2}u_i^\alpha$, $p_0(\chi_0^\alpha + P^\alpha)$, $T_0(1+\theta^\alpha)$, $p_0(\chi_0^\alpha\delta_{ij} + P_{ij}^\alpha)$ and $p_0(2\kappa T_0/m^A)^{1/2}Q_i^\alpha$, where δ_{ij} is the Kronecker delta. Those of the mixture are denoted by $n_0(1+\omega)$, $(2\kappa T_0/m^A)^{1/2}u_i$, $p_0(1+P)$, $T_0(1+\theta)$, $p_0(\delta_{ij} + P_{ij})$ and $p_0(2\kappa T_0/m^A)^{1/2}Q_i$. The definitions of the macroscopic quantities ω^α, u_i^α, etc. in terms of moments of ϕ^α are given in Appendix A. The particle flux of species α flowing between the plates in the X_1-direction per unit width in X_3 and per unit time is denoted by $n_0(2\kappa T_0/m^A)^{1/2}D\chi_0^\alpha M^\alpha$ with

$$M^\alpha = \int_{-1/2}^{1/2} u_1^\alpha \,\mathrm{d}x_2. \tag{2.1}$$

2.2. Similarity solution

It is well known that the solution ϕ^α for the present linear problem can be put in the following form (see Refs. [10, 19]):

$$\begin{aligned}\phi^\alpha = {} & \left\{C_P\chi_0^\alpha + C_T\chi_0^\alpha\left[\hat{m}^\alpha(\zeta_2^2 + \zeta_\rho^2) - \frac{5}{2}\right] \pm C_\chi\right\}x_1 \\ & + \zeta_1\zeta_\rho^{-1}\big[C_P\Phi_P^\alpha(x_2, \zeta_2, \zeta_\rho) + C_T\Phi_T^\alpha(x_2, \zeta_2, \zeta_\rho) + C_\chi\Phi_\chi^\alpha(x_2, \zeta_2, \zeta_\rho)\big],\end{aligned} \tag{2.2}$$

with $\zeta_\rho = \sqrt{\zeta_1^2 + \zeta_3^2}$. Here and henceforth, the double sign $\pm$ (or $\mp$) means $+$ (or $-$) for $\alpha = A$ and $-$ (or $+$) for $\alpha = B$. In the above form, terms containing C_P correspond to the solution for the Poiseuille flow, those containing C_T to the solution for the thermal transpiration and those containing C_χ to the solution for the concentration-driven flow.

The macroscopic quantities ω^α, u_i^α, etc. of species α corresponding to Eq. (2.2) are expressed as follows [see Eq. (A.1) in Appendix A]:

$$\begin{aligned}&\omega^\alpha = (C_P\chi_0^\alpha - C_T\chi_0^\alpha \pm C_\chi)x_1, \\ &u_i^\alpha = \delta_{i1}(C_P u_P^\alpha + C_T u_T^\alpha + C_\chi u_\chi^\alpha), \\ &\theta^\alpha = C_T x_1, \qquad P^\alpha = (C_P\chi_0^\alpha \pm C_\chi)x_1,\end{aligned} \tag{2.3}$$

$$P_{ij}^{\alpha} = \delta_{ij} P^{\alpha} + (\delta_{i1}\delta_{j2} + \delta_{i2}\delta_{j1})(C_P P_P^{\alpha} + C_T P_T^{\alpha} + C_\chi P_\chi^{\alpha}),$$
$$Q_i^{\alpha} = \delta_{i1}(C_P Q_P^{\alpha} + C_T Q_T^{\alpha} + C_\chi Q_\chi^{\alpha}),$$

where u_J^{α}, P_J^{α} and Q_J^{α} $(J = P, T, \chi)$ are written as

$$u_J^{\alpha} = \frac{\pi}{\chi_0^{\alpha}} \int_0^{\infty}\int_{-\infty}^{\infty} \zeta_\rho^2 \Phi_J^{\alpha} E^{\alpha}\, \mathrm{d}\zeta_2\, \mathrm{d}\zeta_\rho,$$
$$P_J^{\alpha} = 2\pi \hat{m}^{\alpha} \int_0^{\infty}\int_{-\infty}^{\infty} \zeta_2 \zeta_\rho^2 \Phi_J^{\alpha} E^{\alpha}\, \mathrm{d}\zeta_2\, \mathrm{d}\zeta_\rho, \tag{2.4}$$
$$Q_J^{\alpha} = \pi \int_0^{\infty}\int_{-\infty}^{\infty} \left[\hat{m}^{\alpha}(\zeta_2^2 + \zeta_\rho^2) - \frac{5}{2}\right] \zeta_\rho^2 \Phi_J^{\alpha} E^{\alpha}\, \mathrm{d}\zeta_2\, \mathrm{d}\zeta_\rho.$$

Similarly, the macroscopic quantities of the mixture are expressed as follows [see Eq. (A.2) in Appendix A]:

$$\omega = (C_P - C_T)x_1, \qquad u_i = \delta_{i1}(C_P u_P + C_T u_T + C_\chi u_\chi),$$
$$\theta = C_T x_1, \qquad P = C_P x_1,$$
$$P_{ij} = \delta_{ij} P + (\delta_{i1}\delta_{j2} + \delta_{i2}\delta_{j1})(C_P P_P + C_T P_T + C_\chi P_\chi), \tag{2.5}$$
$$Q_i = \delta_{i1}(C_P Q_P + C_T Q_T + C_\chi Q_\chi),$$

where u_J, P_J and Q_J $(J = P, T, \chi)$ are written as

$$u_J = \left(\sum_{\beta=A,B} \hat{m}^{\beta} \chi_0^{\beta} u_J^{\beta}\right)\left(\sum_{\beta=A,B} \hat{m}^{\beta} \chi_0^{\beta}\right)^{-1},$$
$$P_J = \sum_{\beta=A,B} P_J^{\beta}, \qquad Q_J = \sum_{\beta=A,B}\left[Q_J^{\beta} - \frac{5}{2}\chi_0^{\beta}(u_J - u_J^{\beta})\right]. \tag{2.6}$$

From Eqs. (2.3) and (2.5), one can see that the pressure p $[= p_0(1 + P)]$ of the mixture and the concentration χ^A $(= \chi_0^A + \omega^A - \chi_0^A \omega)$ of species A are written as $p = p_0(1 + C_P X_1/D)$ and $\chi^A = \chi_0^A + C_\chi X_1/D$ respectively. Therefore, they are independent of X_2 and satisfy the setting of the problem (see Section 2.1). Moreover, one can see that the temperature T $[= T_0(1+\theta)]$ of the mixture is written as $T = T_0(1 + C_T X_1/D)$, which is also independent of X_2 and coincides with the temperature of the plates.

The nondimensional flux M^{α} is written in terms of u_J^{α} as

$$M^{\alpha} = C_P M_P^{\alpha} + C_T M_T^{\alpha} + C_\chi M_\chi^{\alpha},$$
$$M_J^{\alpha} = \int_{-1/2}^{1/2} u_J^{\alpha}\, \mathrm{d}x_2 \quad (J = P, T, \chi). \tag{2.7}$$

2.3. Basic equation and boundary condition

The McCormack model equation [20] (the third order model) for Φ_J^{α} $(J = P, T, \chi)$ can be written in the following form:

$$\zeta_2 \frac{\partial \Phi_J^{\alpha}}{\partial x_2} = \frac{1}{\mathrm{Kn}} \sum_{\beta=A,B} K^{\beta\alpha}(L_J^{\beta\alpha} - C^{\beta\alpha}\Phi_J^{\alpha}) - I_J^{\alpha} \quad (\alpha = A, B), \tag{2.8}$$

with

$$
\begin{aligned}
&L_J^{\beta\alpha} = 2\hat{m}^\alpha \zeta_\rho \left\{ L_{1J}^{\beta\alpha} + \zeta_2 L_{2J}^{\beta\alpha} + \left[\hat{m}^\alpha (\zeta_2^2 + \zeta_\rho^2) - \frac{5}{2} \right] L_{3J}^{\beta\alpha} \right\},\\
&I_P^\alpha = \chi_0^\alpha \zeta_\rho, \qquad I_T^\alpha = \chi_0^\alpha \zeta_\rho \left[\hat{m}^\alpha (\zeta_2^2 + \zeta_\rho^2) - \frac{5}{2} \right], \qquad I_\chi^\alpha = \pm \zeta_\rho,\\
&K^{\beta\alpha} = \left(\frac{d_*^{\beta\alpha}}{d_*^{AA}} \right)^2 \left(\frac{1}{\hat{m}^{\beta\alpha}} \right)^{1/2}, \qquad \hat{m}^{\beta\alpha} = \frac{2\hat{m}^\beta \hat{m}^\alpha}{\hat{m}^\beta + \hat{m}^\alpha},\\
&\mathrm{Kn} = l_0/D, \qquad l_0 = \left[\sqrt{2} \pi n_0 (d_*^{AA})^2 \right]^{-1}.
\end{aligned}
\tag{2.9}
$$

Here $d_*^{\beta\alpha}$ $(= d_*^{\alpha\beta})$ is the reference molecular diameter in β–α collisions, l_0 the reference mean free path of a molecule and Kn the Knudsen number. The definition of $d_*^{\beta\alpha}$ for several molecular models is given in Appendix B. The $L_{iJ}^{\beta\alpha}$ $(i = 1, 2, 3)$ is defined as

$$
L_{1J}^{\beta\alpha} = C^{\beta\alpha} \chi_0^\alpha u_J^\alpha + \chi_0^\alpha \chi_0^\beta (u_J^\beta - u_J^\alpha) \nu_{\beta\alpha}^{(1)} + \left(\frac{\chi_0^\alpha Q_J^\beta}{\hat{m}^\beta} - \frac{\chi_0^\beta Q_J^\alpha}{\hat{m}^\alpha} \right) \nu_{\beta\alpha}^{(2)}, \tag{2.10a}
$$

$$
L_{2J}^{\beta\alpha} = (C^{\beta\alpha} - \chi_0^\beta \nu_{\beta\alpha}^{(3)}) P_J^\alpha + \chi_0^\alpha \nu_{\beta\alpha}^{(4)} P_J^\beta, \tag{2.10b}
$$

$$
L_{3J}^{\beta\alpha} = \frac{2}{5} \left[(C^{\beta\alpha} - \chi_0^\beta \nu_{\beta\alpha}^{(5)}) Q_J^\alpha + \chi_0^\alpha \nu_{\beta\alpha}^{(6)} Q_J^\beta + \frac{5\chi_0^\alpha \chi_0^\beta}{2\hat{m}^\alpha} (u_J^\beta - u_J^\alpha) \nu_{\beta\alpha}^{(2)} \right]. \tag{2.10c}
$$

The $\nu_{\beta\alpha}^{(n)}$ $(n = 1, 2, \ldots, 6)$ are defined as

$$
\begin{aligned}
&\nu_{\beta\alpha}^{(1)} = \frac{8}{3} \frac{\hat{m}^{\beta\alpha}}{\hat{m}^\alpha} \hat{\Omega}_{11}^{\beta\alpha}, \qquad \nu_{\beta\alpha}^{(2)} = \frac{\hat{m}^{\beta\alpha}}{5} \left(\frac{8}{3} \frac{\hat{m}^{\beta\alpha}}{\hat{m}^\alpha} \hat{\Omega}_{12}^{\beta\alpha} - \frac{5}{2} \nu_{\beta\alpha}^{(1)} \right),\\
&\nu_{\beta\alpha}^{(3)} = \frac{\hat{m}^{\beta\alpha}}{\hat{m}^\alpha} \left(\frac{4}{5} \frac{\hat{m}^{\beta\alpha}}{\hat{m}^\alpha} \hat{\Omega}_{22}^{\beta\alpha} + \frac{\hat{m}^\alpha}{\hat{m}^\beta} \nu_{\beta\alpha}^{(1)} \right), \qquad \nu_{\beta\alpha}^{(4)} = \frac{\hat{m}^\alpha}{\hat{m}^\beta} (2\nu_{\beta\alpha}^{(1)} - \nu_{\beta\alpha}^{(3)}),\\
&\nu_{\beta\alpha}^{(5)} = \frac{8}{15} \left(\frac{\hat{m}^{\beta\alpha}}{\hat{m}^\alpha} \right)^3 \frac{\hat{m}^\alpha}{\hat{m}^\beta} \left[\hat{\Omega}_{22}^{\beta\alpha} + \left(\frac{15}{4} \frac{\hat{m}^\alpha}{\hat{m}^\beta} + \frac{25}{8} \frac{\hat{m}^\beta}{\hat{m}^\alpha} \right) \hat{\Omega}_{11}^{\beta\alpha} - \frac{1}{2} \frac{\hat{m}^\beta}{\hat{m}^\alpha} (5\hat{\Omega}_{12}^{\beta\alpha} - \hat{\Omega}_{13}^{\beta\alpha}) \right],\\
&\nu_{\beta\alpha}^{(6)} = \frac{8}{15} \left(\frac{\hat{m}^{\beta\alpha}}{\hat{m}^\alpha} \right)^3 \frac{\hat{m}^\alpha}{\hat{m}^\beta} \left(-\hat{\Omega}_{22}^{\beta\alpha} + \frac{55}{8} \hat{\Omega}_{11}^{\beta\alpha} - \frac{5}{2} \hat{\Omega}_{12}^{\beta\alpha} + \frac{1}{2} \hat{\Omega}_{13}^{\beta\alpha} \right).
\end{aligned}
\tag{2.11}
$$

Here $\hat{\Omega}_{ij}^{\beta\alpha}$ is a nondimensional counterpart of the Chapman–Cowling integral $\Omega_{ij}^{\beta\alpha}$ [Eq. (10.1,1) in Ref. [21]], whose definition and expressions for several molecular models are given in Appendix B. In general, $\hat{\Omega}_{ij}^{\beta\alpha}$ is a function of $\hat{T}_0$ $(= T_0/T_*)$ with T_* being a certain fixed temperature where $d_*^{\beta\alpha}$ is determined [e.g., $d_*^{\beta\alpha}$ for the IPL model is defined by Eq. (B.3) in Appendix B]. The $C^{\beta\alpha}$ is a constant related to the collision frequency between species α and β. It is seen from Eqs. (2.8)–(2.10c) that $C^{\beta\alpha}$ appears only in the form $K^{B\alpha} C^{B\alpha} + K^{A\alpha} C^{A\alpha} (\equiv C^\alpha)$. We adopt the same definition of C^α as that in Ref. [22], which is written as

$$
C^\alpha = \chi_0^\alpha / \hat{\mu}^\alpha. \tag{2.12}
$$

The $\hat{\mu}^\alpha$ is a constant related to the transport coefficient, whose definition is given in Eq. (C.3) in Appendix C.

The boundary condition on the plates at $x_2 = \pm\frac{1}{2}$ is the diffuse reflection condition. In the following, however, we assume $\Phi^\alpha(x_2, \zeta_2, \zeta_\rho) = \Phi^\alpha(-x_2, -\zeta_2, \zeta_\rho)$ making use of the symmetry of the problem and seek the solution in the interval $0 \leqslant x_2 \leqslant \frac{1}{2}$ imposing the specular reflection condition at $x_2 = 0$. That is,

$$
\Phi_J^\alpha = 0 \quad \text{for } \zeta_2 < 0 \text{ at } x_2 = \frac{1}{2}, \tag{2.13a}
$$

$$
\Phi_J^\alpha(0, \zeta_2, \zeta_\rho) = \Phi_J^\alpha(0, -\zeta_2, \zeta_\rho) \quad \text{for } \zeta_2 > 0 \text{ at } x_2 = 0. \tag{2.13b}
$$

The conservation of the momentum in the x_1-direction of the total mixture and the boundary condition (2.13b) lead to the following relations:

$$
P_P = -x_2, \qquad P_T = P_\chi = 0. \tag{2.14}
$$

These relations will be used later to estimate the accuracy of the numerical computations.

2.4. Further reduction

The independent variable ζ_ρ in the boundary-value problem (2.8), (2.13a) and (2.13b) can be eliminated in the same manner as that in Ref. [23]. Let us define the marginal velocity distribution functions F_J^α and G_J^α as

$$\begin{aligned} F_J^\alpha &= \pi \int_0^\infty \zeta_\rho^2 \Phi_J^\alpha E^\alpha \mathrm{d}\zeta_\rho, \\ G_J^\alpha &= \pi \int_0^\infty \zeta_\rho^2 \left(\frac{\hat{m}^\alpha}{2} \zeta_\rho^2 - 1 \right) \Phi_J^\alpha E^\alpha \, \mathrm{d}\zeta_\rho. \end{aligned} \tag{2.15}$$

Integrating Eq. (2.8) multiplied by $\pi\zeta_\rho^2 E^\alpha$ or $\pi\zeta_\rho^2[(\hat{m}^\alpha/2)\zeta_\rho^2 - 1]E^\alpha$ with respect to ζ_ρ over its whole space, we obtain the following equation:

$$\zeta_2 \frac{\partial}{\partial x_2} \begin{bmatrix} F_J^\alpha \\ G_J^\alpha \end{bmatrix} = \frac{1}{\mathrm{Kn}} \left(\begin{bmatrix} L_{FJ}^\alpha \\ L_{GJ}^\alpha \end{bmatrix} - C^\alpha \begin{bmatrix} F_J^\alpha \\ G_J^\alpha \end{bmatrix} \right) - \begin{bmatrix} I_{FJ}^\alpha \\ I_{GJ}^\alpha \end{bmatrix}, \tag{2.16}$$

with

$$\begin{aligned} L_{FJ}^\alpha &= \left[L_{1J}^\alpha + \zeta_2 L_{2J}^\alpha + \left(\hat{m}^\alpha \zeta_2^2 - \frac{1}{2} \right) L_{3J}^\alpha \right] \mathcal{E}^\alpha(\zeta_2), \\ L_{GJ}^\alpha &= L_{3J}^\alpha \mathcal{E}^\alpha(\zeta_2), \end{aligned} \tag{2.17}$$

and

$$\begin{aligned} L_{iJ}^\alpha &= \sum_{\beta=A,B} K^{\beta\alpha} L_{iJ}^{\beta\alpha} \quad (i = 1, 2, 3), \\ \mathcal{E}^\alpha(y) &= \left(\frac{\hat{m}^\alpha}{\pi} \right)^{1/2} \exp(-\hat{m}^\alpha y^2). \end{aligned} \tag{2.18}$$

The inhomogeneous terms I_{FJ}^α and I_{GJ}^α are defined as

$$\begin{aligned} &I_{FP}^\alpha = \frac{\chi_0^\alpha}{2\hat{m}^\alpha} \mathcal{E}^\alpha(\zeta_2), \qquad I_{FT}^\alpha = I_{FP}^\alpha \left(\hat{m}^\alpha \zeta_2^2 - \frac{1}{2} \right), \\ &I_{F\chi}^\alpha = \pm \frac{1}{2\hat{m}^\alpha} \mathcal{E}^\alpha(\zeta_2), \qquad I_{GP}^\alpha = I_{G\chi}^\alpha = 0, \qquad I_{GT}^\alpha = I_{FP}^\alpha. \end{aligned} \tag{2.19}$$

Equation (2.4) for the macroscopic quantities u_J^α, P_J^α and Q_J^α can be recasted in terms of F_J^α and G_J^α as

$$\begin{aligned} u_J^\alpha &= \frac{1}{\chi_0^\alpha} \int_{-\infty}^\infty F_J^\alpha \, \mathrm{d}\zeta_2, \qquad P_J^\alpha = 2\hat{m}^\alpha \int_{-\infty}^\infty \zeta_2 F_J^\alpha \, \mathrm{d}\zeta_2, \\ Q_J^\alpha &= \int_{-\infty}^\infty \left[\left(\hat{m}^\alpha \zeta_2^2 - \frac{1}{2} \right) F_J^\alpha + 2G_J^\alpha \right] \mathrm{d}\zeta_2. \end{aligned} \tag{2.20}$$

The boundary conditions for F_J^α and G_J^α are derived from Eqs. (2.13a) and (2.13b) as

$$\begin{bmatrix} F_J^\alpha \\ G_J^\alpha \end{bmatrix} = 0 \quad \text{for } \zeta_2 < 0 \text{ at } x_2 = \frac{1}{2}, \tag{2.21a}$$

$$\begin{bmatrix} F_J^\alpha \\ G_J^\alpha \end{bmatrix} (0, \zeta_2) = \begin{bmatrix} F_J^\alpha \\ G_J^\alpha \end{bmatrix} (0, -\zeta_2) \quad \text{for } \zeta_2 > 0 \text{ at } x_2 = 0. \tag{2.21b}$$

3. Plan of analysis

In principle, the boundary-value problem (2.16), (2.21a) and (2.21b) can be solved directly and numerically by a standard finite-difference method. However, this direct approach does not work well practically in small or large Knudsen number regimes because of different reasons. Therefore, we carried out the finite-difference analysis only in the intermediate range of the Knudsen number. In small Knudsen number regime, we carried out an asymptotic analysis of the problem and numerically solved the associated Knudsen-layer problem derived in the analysis. In large Knudsen number regime, we considered a system of integral equations for macroscopic quantities that was derived from the above problem (2.16), (2.21a) and (2.21b) and solved it numerically. The analytical expressions for the asymptotic behaviour as $\mathrm{Kn} \to \infty$ were also obtained from this system. The analyses in small and large Knudsen number regimes are described in the following two subsections.

3.1. Asymptotic analysis for small Knudsen numbers

Let us now seek an asymptotic solution of the boundary-value problem (2.16), (2.21a) and (2.21b) for $\mathrm{Kn} \ll 1$ following Sone's asymptotic theory [24,25,9] and its extension to mixtures [26].

3.1.1. Hilbert expansion

To begin with, we seek a moderately varying solution of Eq. (2.16) [i.e., $\partial F_J^\alpha/\partial x_2 = \mathrm{O}(F_J^\alpha)$ and $\partial G_J^\alpha/\partial x_2 = \mathrm{O}(G_J^\alpha)$] by the power series expansion (Hilbert expansion) as follows:

$$h_J^\alpha = h_{J(-1)}^\alpha \mathrm{Kn}^{-1} + h_{J(0)}^\alpha + h_{J(1)}^\alpha \mathrm{Kn} + \cdots \quad (h_J^\alpha = F_J^\alpha,\ G_J^\alpha). \tag{3.1}$$

Correspondingly, the macroscopic quantities are also expanded in the same manner, i.e., Eq. (3.1) with $h_J^\alpha = u_J^\alpha$, P_J^α or Q_J^α. Substituting the above expansion into Eq. (2.16) and equating like powers of Kn, we obtain the following expressions for $F_{J(n)}^\alpha$ and $G_{J(n)}^\alpha$:

$$F_{J(-1)}^\alpha = \chi_0^\alpha u_{J(-1)}^\alpha \mathcal{E}^\alpha(\zeta_2), \qquad G_{J(-1)}^\alpha = 0, \tag{3.2a}$$

$$u_{P(-1)}^\alpha = \frac{1}{2\hat{\mu}}\left(x_2^2 - \frac{1}{4}\right), \qquad u_{T(-1)}^\alpha = u_{\chi(-1)}^\alpha = 0, \tag{3.2b}$$

$$F_{J(0)}^\alpha = (\chi_0^\alpha u_{J(0)}^\alpha + \zeta_2 P_{J(0)}^\alpha)\mathcal{E}^\alpha(\zeta_2), \qquad G_{J(0)}^\alpha = 0, \tag{3.2c}$$

$$u_{P(0)}^\alpha = b_{P(0)}, \qquad u_{T(0)}^\alpha = u_{\chi(0)}^\alpha = 0, \tag{3.2d}$$

$$P_{P(0)}^\alpha = -\frac{\hat{\mu}^\alpha}{\hat{\mu}} x_2, \qquad P_{T(0)}^\alpha = P_{\chi(0)}^\alpha = 0, \tag{3.2e}$$

$$F_{J(1)}^\alpha = \frac{1}{C^\alpha}\left(L_{FJ(1)}^\alpha - I_{FJ}^\alpha - \zeta_2^2 \mathcal{E}^\alpha(\zeta_2)\frac{\partial P_{J(0)}^\alpha}{\partial x_2}\right), \tag{3.2f}$$

$$G_{J(1)}^\alpha = \frac{1}{C^\alpha}(L_{GJ(1)}^\alpha - I_{GJ}^\alpha), \tag{3.2g}$$

$$F_{J(n)}^\alpha = G_{J(n)}^\alpha = 0 \quad (n = 2, 3, \ldots). \tag{3.2h}$$

In the derivation of the above results, Eq. (2.14) and the boundary condition (2.21a) and (2.21b) were partially used (see the last paragraph in this section). The $b_{P(0)}$ in Eq. (3.2d) and $b_{J(1)}$ ($J = P, T, \chi$) appearing later in Eqs. (3.3) and (3.4) are the so-called slip coefficients, which will be determined in the Knudsen-layer analysis explained in the next section. The $\hat{\mu}$ and $\hat{\mu}^\alpha$ in the above and $\hat{D}^\alpha$, $\hat{D}_{AB}$, $\hat{D}_T$ and $\hat{\lambda}^\alpha$ appearing later in Eqs. (3.3)–(3.5) are constants related to the transport coefficients, whose definitions are given in Appendix C. The $L_{FJ(1)}^\alpha$ in Eq. (3.2f) and $L_{GJ(1)}^\alpha$ in Eq. (3.2g) are defined by Eq. (2.17) with u_J^α, P_J^α and Q_J^α replaced, respectively, by $u_{J(1)}^\alpha$, $P_{J(1)}^\alpha$ and $Q_{J(1)}^\alpha$, where $P_{J(1)}^\alpha = 0$ ($J = P, T, \chi$) and the others are given as follows: for $J = P, T$

$$u_{J(1)}^\alpha = b_{J(1)} \mp \frac{1}{2}\Delta_J, \qquad Q_{J(1)}^\alpha = \pm\hat{D}^\alpha \Delta_J + \Upsilon_J^\alpha, \tag{3.3}$$

and for $J = \chi$

$$u^\alpha_{\chi(1)} = b_{\chi(1)} \mp \Delta^\alpha_\chi, \qquad Q^\alpha_{\chi(1)} = \pm \hat{D}^\alpha \frac{\hat{D}_{AB}}{\chi_0^A \chi_0^B}, \tag{3.4}$$

with

$$\begin{aligned}
\Delta_P &= \frac{\hat{D}_{AB}}{\hat{\mu}} \left[\frac{\hat{\mu}^B}{\chi_0^B} \left(1 - \frac{2\hat{D}^B}{5\chi_0^A \chi_0^B} \right) - \frac{\hat{\mu}^A}{\chi_0^A} \left(1 - \frac{2\hat{D}^A}{5\chi_0^A \chi_0^B} \right) \right], \\
\Upsilon^\alpha_P &= \frac{\hat{m}^\beta \Gamma^\beta \hat{\mu}^\alpha + K^{\beta\alpha} \hat{m}^\alpha \chi_0^\alpha \nu^{(6)}_{\beta\alpha} \hat{\mu}^\beta}{2\hat{m}^\alpha \hat{m}^\beta [\Gamma^\alpha \Gamma^\beta - \chi_0^\alpha \chi_0^\beta \nu^{(6)}_{\alpha\beta} \nu^{(6)}_{\beta\alpha} (K^{\beta\alpha})^2] \hat{\mu}}, \\
\Delta_T &= \frac{\hat{D}_T}{\chi_0^A \chi_0^B}, \qquad \Upsilon^\alpha_T = -\hat{\lambda}^\alpha, \\
\Delta^\alpha_\chi &= \left(1 - \frac{\hat{m}^\alpha \chi_0^\alpha}{\chi_0^A + \hat{m}^B \chi_0^B} \right) \frac{\hat{D}_{AB}}{\chi_0^A \chi_0^B}.
\end{aligned} \tag{3.5}$$

Here Γ^α is defined in Eq. (C.3) in Appendix C and $\beta \neq \alpha$ is supposed in the expression for Υ^α_P in Eq. (3.5), i.e., $\beta = B$ for $\alpha = A$ and $\beta = A$ for $\alpha = B$. See the sentence after Eq. (2.2) for the double sign $\pm$ (or $\mp$). It is seen from Eqs. (C.2) and (C.3) in Appendix C that Δ_P, Δ_T and $Q^\alpha_{\chi(1)}$ are finite at $\chi_0^A = 0$ and $\chi_0^B = 0$. The $u^A_{\chi(1)}$ (or $u^B_{\chi(1)}$) diverges at $\chi_0^A = 0$ (or $\chi_0^B = 0$), whereas $\chi_0^A u^A_{\chi(1)}$ (or $\chi_0^B u^B_{\chi(1)}$) remains finite.

The solution $F^\alpha_{J(-1)}$ of $\mathrm{O}(\mathrm{Kn}^{-1})$ was constructed so that it satisfies the boundary condition (2.21a), but $F^\alpha_{P(0)}$ of $\mathrm{O}(\mathrm{Kn}^0)$ and $F^\alpha_{J(1)}$ and $G^\alpha_{J(1)}$ of $\mathrm{O}(\mathrm{Kn}^1)$ were not. In the next section, we will construct the solution which satisfies the condition (2.21a) by introducing a correction in the neighbourhood of the plate which varies in the scale of the mean free path l_0.

3.1.2. Knudsen-layer problem

Here, we seek the solutions which satisfy the boundary condition (2.21a) in the following forms:

$$\begin{aligned}
F^\alpha_P &= F^\alpha_{P(-1)} \mathrm{Kn}^{-1} + (F^\alpha_{P(0)} + f^\alpha_{P(0)}) + (F^\alpha_{P(1)} + f^\alpha_{P(1)}) \mathrm{Kn}, \\
G^\alpha_P &= g^\alpha_{P(0)} + (G^\alpha_{P(1)} + g^\alpha_{P(1)}) \mathrm{Kn}, \\
F^\alpha_J &= (F^\alpha_{J(1)} + f^\alpha_{J(1)}) \mathrm{Kn} \quad (J = T, \chi), \\
G^\alpha_J &= (G^\alpha_{J(1)} + g^\alpha_{J(1)}) \mathrm{Kn} \quad (J = T, \chi).
\end{aligned} \tag{3.6}$$

The $f^\alpha_{J(n)}$ and $g^\alpha_{J(n)}$ are the corrections which are appreciable only in the neighbourhood of the plate and vary in the distance of $\mathrm{O}(l_0)$. In the following, we call $F^\alpha_{J(n)}$ and $G^\alpha_{J(n)}$ the Hilbert part of the solution, and $f^\alpha_{J(n)}$ and $g^\alpha_{J(n)}$ the Knudsen-layer part of the solution. Correspondingly the macroscopic quantities u^α_J, etc. are also expressed as linear combinations of the Hilbert part $u^\alpha_{J(n)}$, etc. and the Knudsen-layer part [see the sentence after Eq. (3.8)].

Let us substitute Eq. (3.6) into Eq. (2.16) and rewrite it in terms of the stretched coordinate η and c defined as

$$\eta = \frac{1}{\mathrm{Kn}} \left(\frac{1}{2} - x_2 \right), \qquad c = -\zeta_2. \tag{3.7}$$

Taking into account the fact that $F^\alpha_{J(n)}$ and $G^\alpha_{J(n)}$ satisfy Eq. (2.16) and the above mentioned assumption for $f^\alpha_{J(n)}$ and $g^\alpha_{J(n)}$ [i.e., $\partial f^\alpha_{J(n)}/\partial\eta = \mathrm{O}(f^\alpha_{J(n)})$ and $\partial g^\alpha_{J(n)}/\partial\eta = \mathrm{O}(g^\alpha_{J(n)})$], we obtain the following equation: for $(J, n) = (P, 0)$, $(P, 1)$, $(T, 1)$ and $(\chi, 1)$

$$c \frac{\partial}{\partial\eta} \begin{bmatrix} f^\alpha_{J(n)} \\ g^\alpha_{J(n)} \end{bmatrix} = \begin{bmatrix} \mathcal{L}^\alpha_{fJ(n)} \\ \mathcal{L}^\alpha_{gJ(n)} \end{bmatrix} - C^\alpha \begin{bmatrix} f^\alpha_{J(n)} \\ g^\alpha_{J(n)} \end{bmatrix}. \tag{3.8}$$

Here $\mathcal{L}^\alpha_{fJ(n)}$ and $\mathcal{L}^\alpha_{gJ(n)}$ are defined by Eq. (2.17) with ζ_2 replaced by c and the macroscopic quantities u^α_J, P^α_J and Q^α_J by their Knudsen-layer parts $U^\alpha_{J(n)}$, $S^\alpha_{J(n)}$ and $W^\alpha_{J(n)}$ respectively. Those Knudsen-layer parts are defined by Eq. (2.20)

with ζ_2, F_J^α and G_J^α being replaced by c, $f_{J(n)}^\alpha$ and $g_{J(n)}^\alpha$. The boundary conditions for $f_{J(n)}^\alpha$ and $g_{J(n)}^\alpha$ can be derived from Eq. (2.21a) and the assumption that $f_{J(n)}^\alpha$ and $g_{J(n)}^\alpha$ are appreciable only in the neighbourhood of the plate:

$$\begin{bmatrix} f_{J(n)}^\alpha \\ g_{J(n)}^\alpha \end{bmatrix} = \begin{bmatrix} -F_{J(n)}^\alpha \\ -G_{J(n)}^\alpha \end{bmatrix} \quad \text{for } c > 0 \text{ at } \eta = 0, \tag{3.9a}$$

$$\begin{bmatrix} f_{J(n)}^\alpha \\ g_{J(n)}^\alpha \end{bmatrix} \to \begin{bmatrix} 0 \\ 0 \end{bmatrix} \quad \text{as } \eta \to \infty, \tag{3.9b}$$

with $F_{J(n)}^\alpha$ and $G_{J(n)}^\alpha$ in the right-hand side of Eq. (3.9a) being evaluated at $x_2 = \frac{1}{2}$. We shall call the half-space problem (3.8), (3.9a) and (3.9b) the Knudsen-layer problem [27].[2] In this problem, corresponding to Eq. (2.14), the conservation law and the boundary condition (3.9b) lead to

$$S_{J(n)}(\equiv S_{J(n)}^A + S_{J(n)}^B) = 0. \tag{3.10}$$

This relation will be used later to estimate the accuracy of the numerical computations.

3.1.3. Expressions for the particle fluxes

As mentioned after Eq. (3.6), the flow velocity u_J^α is expressed as a linear combination of the Hilbert part $u_{J(n)}^\alpha$ and the Knudsen-layer part $U_{J(n)}^\alpha$. Correspondingly the particle flux M_J^α is also expressed as the sum of the contribution of the Hilbert part M_{HJ}^α and that of the Knudsen-layer part M_{KJ}^α:

$$M_J^\alpha = M_{HJ}^\alpha + M_{KJ}^\alpha. \tag{3.11}$$

The M_{HJ}^α is obtained by the integration of $u_{J(n)}^\alpha$ in Eqs. (3.2b), (3.2d), (3.3) and (3.4):

$$\begin{aligned} M_{HP}^\alpha &= -\frac{1}{12\hat{\mu}\mathrm{Kn}} + b_{P(0)} + \left(b_{P(1)} \mp \frac{1}{2}\Delta_P\right)\mathrm{Kn}, \\ M_{HT}^\alpha &= \left(b_{T(1)} \mp \frac{1}{2}\Delta_T\right)\mathrm{Kn}, \\ M_{H\chi}^\alpha &= (b_{\chi(1)} \mp \Delta_\chi^\alpha)\mathrm{Kn}. \end{aligned} \tag{3.12}$$

The M_{KJ}^α is expressed as follows:

$$\begin{aligned} M_{KP}^\alpha &= (\mathcal{M}_{P(0)}^\alpha + \mathcal{M}_{P(1)}^\alpha \mathrm{Kn})\mathrm{Kn}, \\ M_{KJ}^\alpha &= \mathcal{M}_{J(1)}^\alpha \mathrm{Kn}^2 \quad (J = T, \chi), \end{aligned} \tag{3.13}$$

with

$$\mathcal{M}_{J(n)}^\alpha = 2\int_0^\infty U_{J(n)}^\alpha \,\mathrm{d}\eta. \tag{3.14}$$

The slip coefficient $b_{J(n)}$ in Eq. (3.12) and $\mathcal{M}_{J(n)}^\alpha$ in Eq. (3.13) are obtained by the analysis of the Knudsen-layer problem (3.8), (3.9a) and (3.9b).

3.2. Analysis for large Knudsen numbers based on integral equations

When the Knudsen number becomes large, the solution F_J^α and G_J^α of the boundary-value problem (2.16), (2.21a) and (2.21b) localizes to the neighbourhood of $\zeta_2 = 0$ in the ζ_2-space and shows abrupt change around there. Such behaviour of the velocity distribution function is clearly shown in Refs. [10,19], where the problem was analyzed on

[2] The boundary condition (3.9a) contains an undetermined constant (the slip coefficient) $b_{J(n)}$ [see Eqs. (3.2c)–(3.2g), (3.3) and (3.4)]. In the case of the linearized Boltzmann equation for hard-sphere molecules, it is proved in Ref. [27] that the Knudsen-layer problem has a unique solution if and only if the slip coefficient takes a special value and the solution decays exponentially as $\eta \to \infty$. We assume that the same holds in the present analysis based on the McCormack model.

the basis of the original Boltzmann equation. Consequently, we must use finer grid points in ζ_2 around $\zeta_2 = 0$ to carry out accurate computations for larger values of Kn. In order to bypass this difficulty, we consider the transformation of the problem into a system of integral equations for macroscopic quantities and make use of it in the analysis for large Knudsen numbers.

In this section, we first derive a system of integral equations for macroscopic quantities from the problem (2.16), (2.21a) and (2.21b). Then we derive the explicit expressions of the macroscopic quantities for $\mathrm{Kn} \to \infty$ from the integral equations, following the similar analyses in the case of single-component gases in Refs. [28–30].

3.2.1. Integral equations for macroscopic quantities

The solution F_J^α for fixed $\zeta_2(\neq 0)$ of the boundary-value problem (2.16), (2.21a) and (2.21b) may formally be written as

$$F_J^\alpha = \frac{1}{\zeta_2 \mathrm{Kn}} \int_{x_w}^{x_2} \exp\left(\frac{C^\alpha}{\zeta_2 \mathrm{Kn}}(s - x_2)\right) L_{FJ}^\alpha(s; \zeta_2)\, \mathrm{d}s - \frac{\mathrm{Kn}}{C^\alpha} I_{FJ}^\alpha \left[1 - \exp\left(\frac{C^\alpha}{\zeta_2 \mathrm{Kn}}(x_w - x_2)\right)\right], \tag{3.15}$$

where $x_w = \mp\frac{1}{2}$ for $\zeta_2 \gtrless 0$. In the above expression, L_{FJ}^α is defined by Eq. (2.17) and has a property $L_{FJ}^\alpha(x_2; \zeta_2) = L_{FJ}^\alpha(-x_2; -\zeta_2)$ owing to the assumption made in the second paragraph in Section 2.3. A similar formal solution for G_J^α can be derived, but is omitted for conciseness.

Substituting the above results for F_J^α and G_J^α into Eq. (2.20), we have a system of integral equations for u_J^α, P_J^α and Q_J^α:

$$\begin{aligned}
\chi_0^\alpha u_J^\alpha = {} & I_{UJ}^\alpha + \frac{1}{C^\alpha} \int_0^{1/2} \Delta_G\left(s + x_2, s - x_2; \frac{\tilde{C}^\alpha}{\mathrm{Kn}}\right)\left[L_{1J}^\alpha(s) - \frac{1}{2} L_{3J}^\alpha(s)\right] \mathrm{d}s \\
& - \frac{1}{\mathrm{Kn}} \int_0^{1/2} \Delta_0''\left(s + x_2, s - x_2; \frac{\tilde{C}^\alpha}{\mathrm{Kn}}\right) L_{2J}^\alpha(s)\, \mathrm{d}s \\
& + \frac{\sqrt{\hat{m}^\alpha}}{\mathrm{Kn}} \int_0^{1/2} \Delta_1\left(s + x_2, s - x_2; \frac{\tilde{C}^\alpha}{\mathrm{Kn}}\right) L_{3J}^\alpha(s)\, \mathrm{d}s,
\end{aligned} \tag{3.16a}$$

$$\begin{aligned}
\frac{1}{2\hat{m}^\alpha} P_J^\alpha = {} & I_{PJ}^\alpha + \frac{1}{\mathrm{Kn}} \int_0^{1/2} \bar{\Delta}_0''\left(s + x_2, s - x_2; \frac{\tilde{C}^\alpha}{\mathrm{Kn}}\right)\left[L_{1J}^\alpha(s) - \frac{1}{2} L_{3J}^\alpha(s)\right] \mathrm{d}s \\
& - \frac{1}{\mathrm{Kn}\sqrt{\hat{m}^\alpha}} \int_0^{1/2} \bar{\Delta}_1\left(s + x_2, s - x_2; \frac{\tilde{C}^\alpha}{\mathrm{Kn}}\right) L_{2J}^\alpha(s)\, \mathrm{d}s \\
& + \frac{1}{\mathrm{Kn}} \int_0^{1/2} \bar{\Delta}_2''\left(s + x_2, s - x_2; \frac{\tilde{C}^\alpha}{\mathrm{Kn}}\right) L_{3J}^\alpha(s)\, \mathrm{d}s,
\end{aligned} \tag{3.16b}$$

$$\begin{aligned}
Q_J^\alpha + \frac{1}{2}\chi_0^\alpha u_J^\alpha = {} & I_{QJ}^\alpha + \frac{2}{C^\alpha} \int_0^{1/2} \Delta_G\left(s + x_2, s - x_2; \frac{\tilde{C}^\alpha}{\mathrm{Kn}}\right) L_{3J}^\alpha(s)\, \mathrm{d}s \\
& + \frac{\sqrt{\hat{m}^\alpha}}{\mathrm{Kn}} \int_0^{1/2} \Delta_1\left(s + x_2, s - x_2; \frac{\tilde{C}^\alpha}{\mathrm{Kn}}\right)\left[L_{1J}^\alpha(s) + \frac{1}{2} L_{3J}^\alpha(s)\right] \mathrm{d}s
\end{aligned}$$

$$- \frac{1}{\mathrm{Kn}} \int_0^{1/2} \Delta_2'' \left(s + x_2, s - x_2; \frac{\tilde{C}^\alpha}{\mathrm{Kn}} \right) L_{2J}^\alpha(s)\, \mathrm{d}s$$

$$+ \frac{\hat{m}^\alpha C^\alpha}{2\mathrm{Kn}^2} \int_0^{1/2} \Delta_0' \left(s + x_2, s - x_2; \frac{\tilde{C}^\alpha}{\mathrm{Kn}} \right) L_{3J}^\alpha(s)\, \mathrm{d}s, \tag{3.16c}$$

with $\tilde{C}^\alpha = \sqrt{\hat{m}^\alpha} C^\alpha$ and

$$\begin{aligned}
I_{UP}^\alpha &= \frac{\chi_0^\alpha \mathrm{Kn}}{2\hat{m}^\alpha C^\alpha} \left[-1 + \Delta_0 \left(\frac{1}{2} + x_2, \frac{1}{2} - x_2; \frac{\tilde{C}^\alpha}{\mathrm{Kn}} \right) \right], \\
I_{PP}^\alpha &= \frac{\chi_0^\alpha \mathrm{Kn}}{2(\hat{m}^\alpha)^{3/2} C^\alpha} \bar{\Delta}_1 \left(\frac{1}{2} + x_2, \frac{1}{2} - x_2; \frac{\tilde{C}^\alpha}{\mathrm{Kn}} \right), \\
I_{QP}^\alpha &= \frac{\chi_0^\alpha \mathrm{Kn}}{4\hat{m}^\alpha C^\alpha} \left[-1 + 2\Delta_2 \left(\frac{1}{2} + x_2, \frac{1}{2} - x_2; \frac{\tilde{C}^\alpha}{\mathrm{Kn}} \right) \right], \\
I_{UT}^\alpha &= -\frac{1}{2} I_{UP}^\alpha + I_{QP}^\alpha, \\
I_{PT}^\alpha &= \frac{1}{2} I_{PP}^\alpha + \frac{\chi_0^\alpha}{4\hat{m}^\alpha} \bar{\Delta}_0' \left(\frac{1}{2} + x_2, \frac{1}{2} - x_2; \frac{\tilde{C}^\alpha}{\mathrm{Kn}} \right), \\
I_{QT}^\alpha &= 2I_{UP}^\alpha + I_{QP}^\alpha + \frac{\chi_0^\alpha}{4\sqrt{\hat{m}^\alpha}} \Delta_1' \left(\frac{1}{2} + x_2, \frac{1}{2} - x_2; \frac{\tilde{C}^\alpha}{\mathrm{Kn}} \right), \\
I_{U\chi}^\alpha &= \pm \frac{1}{\chi_0^\alpha} I_{UP}^\alpha, \qquad I_{P\chi}^\alpha = \pm \frac{1}{\chi_0^\alpha} I_{PP}^\alpha, \qquad I_{Q\chi}^\alpha = \pm \frac{1}{\chi_0^\alpha} I_{QP}^\alpha.
\end{aligned} \tag{3.17}$$

See the sentence after Eq. (2.2) for the double sign $\pm$. The Δ_G, Δ_n $(n = 0, 1, 2)$, etc. in Eqs. (3.16a)–(3.16c) and (3.17) are expressed in terms of the Abramowitz function J_n [31] as

$$\begin{aligned}
&\pi^{1/2} \Delta_n(s, t; a) = J_n(as) + J_n\big(a|t|\big), \\
&\pi^{1/2} \bar{\Delta}_n(s, t; a) = J_n(as) - J_n\big(a|t|\big), \\
&\pi^{1/2} \Delta_n'(s, t; a) = s J_n(as) + |t| J_n\big(a|t|\big), \\
&\pi^{1/2} \bar{\Delta}_n'(s, t; a) = s J_n(as) - |t| J_n\big(a|t|\big), \\
&\pi^{1/2} \Delta_n''(s, t; a) = J_n(as) + \mathrm{sign}(t) J_n\big(a|t|\big), \\
&\bar{\Delta}_n''(s, t; a) = \Delta_n''(s, -t; a), \\
&\pi^{1/2} \Delta_G(s, t; a) = G(s; a) + G\big(|t|; a\big),
\end{aligned} \tag{3.18}$$

where $\mathrm{sign}(t) = \pm 1$ for $t \gtrless 0$ and

$$\begin{aligned}
J_n(s) &= \int_0^\infty t^n \exp\left(-t^2 - \frac{s}{t} \right) \mathrm{d}t, \\
G(s; a) &= \frac{2J_2(as) - J_0(as)}{s}.
\end{aligned} \tag{3.19}$$

Some properties of J_n [Eqs. (27.5.2) and (27.5.3) in Ref. [31]] were used in the derivation of Eqs. (3.16a)–(3.16c) and (3.17).

It should be noted here that essentially the same integral equations have been derived and solved by means of the variational method of approximative nature in Ref. [12]. In contrast, we performed straightforward computations to obtain more reliable solutions (see Section 5.3 for the details).

3.2.2. Asymptotic analysis for large Knudsen numbers

We now investigate the asymptotic behaviour of the mixture for $\mathrm{Kn} \to \infty$. The following power series representation for the Abramowitz function J_n can be derived from Eqs. (27.5.2)–(27.5.4) in Ref. [31]:

$$\begin{aligned} J_0(s) &= \frac{\pi^{1/2}}{2} - \left(1 - \frac{3}{2}\gamma\right)s + s\ln s - \frac{\pi^{1/2}}{2}s^2 + \cdots, \\ J_1(s) &= \frac{1}{2} - \frac{\pi^{1/2}}{2}s + \frac{3}{4}(1-\gamma)s^2 + \cdots, \\ J_2(s) &= \frac{\pi^{1/2}}{4} - \frac{1}{2}s + \frac{\pi^{1/2}}{4}s^2 + \cdots, \end{aligned} \tag{3.20}$$

where $\gamma (= 0.577\,216)$ is the Euler constant. Substituting the above expansions into Eq. (3.18), one can see that the integral kernels and the inhomogeneous terms in Eqs. (3.16a)–(3.16c) are expressed in the following expansions:

$$\begin{aligned} V(\mathrm{Kn}) &= (\mathrm{Kn}^{-1}\ln\mathrm{Kn})V^{(0)} + \mathrm{Kn}^{-1}V^{(1)} + \mathrm{O}(\mathrm{Kn}^{-2}\ln\mathrm{Kn}), \\ I(\mathrm{Kn}) &= (\ln\mathrm{Kn})I^{(0)} + I^{(1)} + \mathrm{O}(\mathrm{Kn}^{-1}\ln\mathrm{Kn}), \end{aligned} \tag{3.21}$$

where $V(\mathrm{Kn})$ represents the integral kernels Δ_G/C^α, Δ_0''/Kn, $(\sqrt{\hat{m}^\alpha}/\mathrm{Kn})\Delta_1$, etc. and $I(\mathrm{Kn})$ the inhomogeneous terms I^α_{UJ}, I^α_{PJ} and I^α_{QJ}. Then, bearing in mind the structure of Eqs. (3.16a)–(3.16c), one obtains

$$U = (\ln\mathrm{Kn})I^{(0)} + I^{(1)} + \mathrm{O}\big[\mathrm{Kn}^{-1}(\ln\mathrm{Kn})^2\big], \tag{3.22}$$

where U represents the left-hand sides of the integral equations (3.16a)–(3.16c). Equation (3.22) means that $\chi_0^\alpha u_J^\alpha$, $P_J^\alpha/2\hat{m}^\alpha$ and $Q_J^\alpha + \chi_0^\alpha u_J^\alpha/2$ coincide, respectively, with I^α_{UJ}, I^α_{PJ} and I^α_{QJ} up to the second term of the expansion. As a result, the macroscopic quantities for $\mathrm{Kn} \to \infty$ are given as follows:

$$\begin{aligned} &u_P^\alpha \sim \frac{1}{2\sqrt{\pi\hat{m}^\alpha}}\left[-\ln\mathrm{Kn} - 1 + \frac{3}{2}\gamma + \ln\big(\sqrt{\hat{m}^\alpha}C^\alpha\big) + \left(\frac{1}{2}+x_2\right)\ln\left(\frac{1}{2}+x_2\right) + \left(\frac{1}{2}-x_2\right)\ln\left(\frac{1}{2}-x_2\right)\right], \\ &P_P^\alpha \sim -\chi_0^\alpha x_2, \qquad Q_P^\alpha + \frac{1}{2}\chi_0^\alpha u_P^\alpha \sim -\frac{\chi_0^\alpha}{4\sqrt{\pi\hat{m}^\alpha}}, \\ &u_T^\alpha \sim -\frac{1}{2}u_P^\alpha - \frac{1}{4\sqrt{\pi\hat{m}^\alpha}}, \qquad P_T^\alpha \sim 0, \qquad Q_T^\alpha \sim \frac{9}{4}\chi_0^\alpha u_P^\alpha, \\ &\chi_0^\alpha u_\chi^\alpha \sim \pm u_P^\alpha, \qquad P_\chi^\alpha \sim \mp x_2, \qquad Q_\chi^\alpha + \frac{1}{2}\chi_0^\alpha u_\chi^\alpha \sim \mp\frac{1}{4\sqrt{\pi\hat{m}^\alpha}}. \end{aligned} \tag{3.23}$$

Integrating u_P^α, u_T^α and u_χ^α in Eq. (3.23), we have

$$\begin{aligned} M_P^\alpha &= \frac{1}{2\sqrt{\pi\hat{m}^\alpha}}\left[-\ln\mathrm{Kn} - \frac{3}{2}(1-\gamma) + \ln\big(\sqrt{\hat{m}^\alpha}C^\alpha\big)\right] + \mathrm{O}\big[\mathrm{Kn}^{-1}(\ln\mathrm{Kn})^2\big], \\ M_T^\alpha &= \frac{1}{4\sqrt{\pi\hat{m}^\alpha}}\left[\ln\mathrm{Kn} + \frac{1}{2}(1-3\gamma) - \ln\big(\sqrt{\hat{m}^\alpha}C^\alpha\big)\right] + \mathrm{O}\big[\mathrm{Kn}^{-1}(\ln\mathrm{Kn})^2\big], \\ \chi_0^\alpha M_\chi^\alpha &= \pm\frac{1}{2\sqrt{\pi\hat{m}^\alpha}}\left[-\ln\mathrm{Kn} - \frac{3}{2}(1-\gamma) + \ln\big(\sqrt{\hat{m}^\alpha}C^\alpha\big)\right] + \mathrm{O}\big[\mathrm{Kn}^{-1}(\ln\mathrm{Kn})^2\big]. \end{aligned} \tag{3.24}$$

4. Database of the particle fluxes

In the present work, we consider the following two kinds of mixture: (i) mixtures of virtual gases composed of the hard-sphere (HS) or Maxwell molecules and (ii) mixtures of noble gases, i.e., He–Ne, He–Ar and Ne–Ar. In the latter case, we assume the HS, Maxwell, inverse-power-law (IPL) potential and Lennard-Jones (LJ) 12,6 molecular models. For those mixtures, we carried out the analyses described in the previous sections and constructed the databases of the particle fluxes M_J^α $(J = P, T, \chi; \alpha = A, B)$.

In this section, we first show the method of the database construction and then show the behaviour of M_J^α obtained by the databases. The behaviour of the macroscopic quantities u_J^α, etc. and that of the velocity distribution functions will be omitted for conciseness (see Refs. [16,17,19] for them).

4.1. Construction of the database

We first note that if one specifies the substances of the component gases, i.e., parameters concerning the properties of molecules or molecular interactions such as m^α, $d_*^{\beta\alpha}$, etc. (see Appendix B and Table 1 appearing later), the boundary-value problem (2.16), (2.21a) and (2.21b) [or the system (3.16a)–(3.16c)] is characterized by Kn, χ_0^A and $\hat{T}_0$ ($= T_0/T_*$) [Chapman–Cowling's integral in Eq. (2.11) is a function of $\hat{T}_0$; see Appendix B]. Therefore, the particle flux M_J^α is a function of those three parameters.

Let us first construct a database of M_J^α for fixed $\hat{T}_0$ using the Chebyshev polynomial approximation with respect to Kn and χ_0^A following Ref. [32]. Let C_n be the Chebyshev polynomial of order n, which can be defined by [33]

$$C_n(\cos\theta) = \cos n\theta \quad (0 \leqslant \theta \leqslant \pi). \tag{4.1}$$

The M_J^α for fixed $\hat{T}_0$ is approximated by C_n in the interval $\mathrm{K}_0 \leqslant \mathrm{Kn} \leqslant \mathrm{K}_1$ and $0 \leqslant \chi_0^A \leqslant 1$ as [33]

$$M_J^\alpha(\mathrm{Kn}, \chi_0^A, \hat{T}_0) = \sum_{m=0}^{N_\mathrm{K}} \sum_{n=0}^{N_\chi} a_{mn}(\hat{T}_0) C_m\left(\frac{2\ln \mathrm{Kn} - \ln(\mathrm{K}_1\mathrm{K}_0)}{\ln(\mathrm{K}_1/\mathrm{K}_0)}\right) C_n(2\chi_0^A - 1). \tag{4.2}$$

The coefficients a_{mn} are written as

$$\begin{aligned} a_{mn}(\hat{T}_0) = {} & \frac{1}{N_\mathrm{K} N_\chi \bar{\epsilon}_m \epsilon_n} \sum_{i=0}^{N_\mathrm{K}-1} \sum_{j=0}^{N_\chi-1} \big(M^\alpha_{J(i,j)}(\hat{T}_0) C_m(\bar{s}_i) C_n(s_j) + M^\alpha_{J(i,j+1)}(\hat{T}_0) C_m(\bar{s}_i) C_n(s_{j+1}) \\ & + M^\alpha_{J(i+1,j)}(\hat{T}_0) C_m(\bar{s}_{i+1}) C_n(s_j) + M^\alpha_{J(i+1,j+1)}(\hat{T}_0) C_m(\bar{s}_{i+1}) C_n(s_{j+1}) \big), \end{aligned} \tag{4.3}$$

with $\bar{\epsilon}_0 = \bar{\epsilon}_{N_\mathrm{K}} = 2$, $\bar{\epsilon}_1 = \cdots = \bar{\epsilon}_{N_\mathrm{K}-1} = 1$, $\epsilon_0 = \epsilon_{N_\chi} = 2$, $\epsilon_1 = \cdots = \epsilon_{N_\chi - 1} = 1$ and

$$M^\alpha_{J(i,j)}(\hat{T}_0) = M_J^\alpha\left(\frac{\ln(\mathrm{K}_1/\mathrm{K}_0)}{2}\bar{s}_i + \frac{\ln(\mathrm{K}_1\mathrm{K}_0)}{2}, \frac{s_j + 1}{2}, \hat{T}_0\right), \tag{4.4a}$$

$$\bar{s}_i = \cos\left(i\frac{\pi}{N_\mathrm{K}}\right) \quad (i = 0, 1, \ldots, N_\mathrm{K}), \tag{4.4b}$$

$$s_j = \cos\left(j\frac{\pi}{N_\chi}\right) \quad (j = 0, 1, \ldots, N_\chi). \tag{4.4c}$$

The above $M^\alpha_{J(i,j)}$ are obtained by the analyses of the problem (2.16), (2.21a) and (2.21b) [or (3.16a)–(3.16c)] for $(N_\mathrm{K}+1)\times(N_\chi+1)$ pairs of the parameters (Kn, χ_0^A) corresponding to the Chebyshev abscissa. The coefficients a_{mn} are obtained by Eq. (4.3) and stored as a database. Then, M_J^α at arbitrary values of Kn ($\mathrm{K}_0 \leqslant \mathrm{Kn} \leqslant \mathrm{K}_1$) and χ_0^A is given promptly by the formula (4.2).

The M_J^α for small Kn is given by Eqs. (3.11)–(3.14). The $b_{J(n)}$ (the slip coefficients) and $\mathcal{M}^\alpha_{J(n)}$ defined by Eq. (3.14) are determined by the analysis of the Knudsen-layer problem (3.8), (3.9a) and (3.9b) and are functions of $(\chi_0^A, \hat{T}_0)$ in this case. The databases of $b_{J(n)}$ and $\mathcal{M}^\alpha_{J(n)}$ for fixed $\hat{T}_0$ can be constructed by use of the Chebyshev polynomial approximation with respect to χ_0^A in a similar manner as that described above.

Such databases of M_J^α, $b_{J(n)}$ and $\mathcal{M}^\alpha_{J(n)}$ are to be constructed at several different values of $\hat{T}_0$ in a certain range $\hat{T}_\mathrm{min} \leqslant \hat{T}_0 \leqslant \hat{T}_\mathrm{max}$. Then, one can obtain M_J^α at an arbitrary value of $\hat{T}_0$ in that range by means of the spline interpolation.

Electronic files of the databases and FORTRAN codes which reproduce the values of M_J^α at arbitrary values of Kn and χ_0^A in a wide range of $\hat{T}_0$ are available as Electronic Annex 2 in the online version of this article. As explained in Section 1, those databases can be readily incorporated in the fluid-dynamic models for practical channel-flow problems. For instance, one can investigate the behaviour of a binary mixture in a stationary nonisothermal plane channel or in the Knudsen compressor by use of the fluid-dynamic model in Ref. [3] with the databases constructed above [$\mathcal{M}_J^\alpha(\mathrm{K}, \chi^\mathrm{A}_{(0)}, \hat{T}_\mathrm{w})$ in Ref. [3] is equivalent with $M_J^\alpha(\mathrm{Kn}, \chi_0^A, \hat{T}_0)$ in the present work with $\mathrm{Kn} = \mathrm{K}$, $\chi_0^A = \chi^\mathrm{A}_{(0)}$ and $\hat{T}_0 = \hat{T}_\mathrm{w}$]. Other examples illustrating how to use the flux database are found, e.g., in Refs. [1,7] in the case of the generalized Reynolds equation for the gas film lubrication problems and in Ref. [2] in the case of the degenerated

Reynolds equation for the microchannel flow problems, although those references are concerned with the case of a single-component gas.

4.2. Results for virtual gas mixtures

We carried out the analyses for virtual gas mixtures with $m^B/m^A = 2$, 4 and 10, and $d^B/d^A = 1$ for hard-sphere (HS) molecules (d^α is the molecular diameter of species α) and $d_*^{BB}/d_*^{AA} = d_*^{BA}/d_*^{AA} = 1$ for the Maxwell molecules. It should be noted that M_J^α for the HS molecules are independent of $\hat{T}_0$, whereas that for the Maxwell molecules depends on it and satisfies the following relation (see Appendix B):

$$M_J^\alpha(\mathrm{Kn}, \chi_0^A, \hat{T}_0) = M_J^\alpha\big(\mathrm{Kn}\sqrt{\hat{T}_0}, \chi_0^A, 1\big). \tag{4.5}$$

That is, M_J^α at an arbitrary value of $\hat{T}_0$ can be obtained from that at $\hat{T}_0 = 1$ by the transformation of Kn. Therefore, the analyses for the Maxwell molecules were carried out only at $\hat{T}_0 = 1$.

The particle flux M_J^α for HS is shown as a function of Kn in Fig. 1. The M_T^A and M_T^B of the thermal transpiration and $|M_\chi^A|$ and M_χ^B of the concentration-driven flow grow monotonically for increasing Kn. In the meantime, $|M_P^A|$ and $|M_P^B|$ of the Poiseuille flow have their minimums at $\mathrm{Kn} \sim 1$, which is a phenomenon well known as the Knudsen minimum (see, e.g., Ref. [34]). The difference between M_P^A and M_P^B tends to vanish as Kn decreases, because the Hilbert part M_{HP}^α up to $\mathrm{O}(\mathrm{Kn}^0)$ is common to both species [see Eq. (3.12)].

In Fig. 1, the results of the linearized Boltzmann equation obtained in Ref. [19] are also shown for comparison. As can be seen in the figure, the McCormack model reproduces well the results of the Boltzmann equation, especially when Kn is small. This reflects the fact that those two equations give the same expressions for the transport coefficients at their first or second approximations in the Chapman–Enskog theory (see Appendix C and Ref. [21]).

Figure 2 shows the results for the Maxwell molecules. As is well known, the thermal–diffusion coefficient is zero, i.e., $\hat{D}_T = 0$ (see Appendix C) in the case of the Maxwell molecules. Consequently, the difference between M_T^A and M_T^B tends to vanish as Kn decreases [see Eqs. (3.12) and (3.5)].

We should stress that the databases constructed and provided as Electronic Annex 2 can reproduce values of M_J^α's in the entire range of Kn and χ_0^A, whereas their behaviour only at $\chi_0^A = 0.5$ in the limited range of Kn is shown in Figs. 1 and 2. Supplementary figure and more detailed numerical data are presented as Fig. 1 and Tables 1–18 in Electronic Annex 1 in the online version of this article.

4.3. Results for mixtures of noble gases

We carried out the analyses for mixtures of noble gases, i.e., He–Ne, He–Ar and Ne–Ar, assuming the hard-sphere (HS), Maxwell, inverse power-law (IPL) potential and Lennard-Jones (LJ) 12,6 molecular models. The molar weight of He, Ne and Ar are 4.003, 20.183 and 39.944 respectively. The other data of the molecules (see Appendix B) used in the present work were mainly cited from Ref. [21] and are listed in Table 1.

The data in Table 1 concerning the molecular interactions between the same species are determined from the viscosity and those between the different species are from the mutual diffusion coefficient. In particular, we determined $d_*^{\beta\alpha}$ of the Maxwell and IPL model by equating the first approximation $[\mu]_1$ of the viscosity and $[D_{12}]_1$ of the mutual diffusion coefficient in the Chapman–Enskog theory [see Eqs. (9.7,3) and (9.81,1) in Ref. [21]] to their experimental values measured at temperature $T_* = 273$K. Incidentally, the diameter of a HS molecule in Table 1, which was cited from Ref. [21], is determined from an experimental value of the viscosity measured at the same temperature. As a result, using the data in Table 1, one reproduces values of the viscosity and mutual diffusion coefficient (or Ω_{22}^{AA}, Ω_{22}^{BB} and Ω_{11}^{BA}) which are almost common to all the molecular models at temperature $T_0(= T_*) = 273$ K. However, they differ each other at other temperatures ($T_0 \neq T_*$), since the temperature dependence of the transport coefficients (or $\Omega_{ij}^{\beta\alpha}$) is different for respective molecular models.

Figures 3–5 show M_J^α for the mixture of He (species A) and Ne (species B) in the case of $\chi_0^A = 0.5$ as a function of the Knudsen number: Fig. 3 is for $\hat{T}_0 = 1$ (or $T_0 = 273$ K), Fig. 4 for $\hat{T}_0 = 2$ ($T_0 = 546$ K) and Fig. 5 for $\hat{T}_0 = 0.5$ ($T_0 = 136.5$ K). Here we introduce $d_0 = 2.193 \times 10^{-8}$cm as the reference molecular diameter for He–Ne mixture, which is common to all the molecular models, and define $\mathrm{Kn}' = a\mathrm{Kn}$ with $a = (d_*^{AA}/d_0)^2$ [i.e., $a = 1$(HS), 1.38(Maxwell),

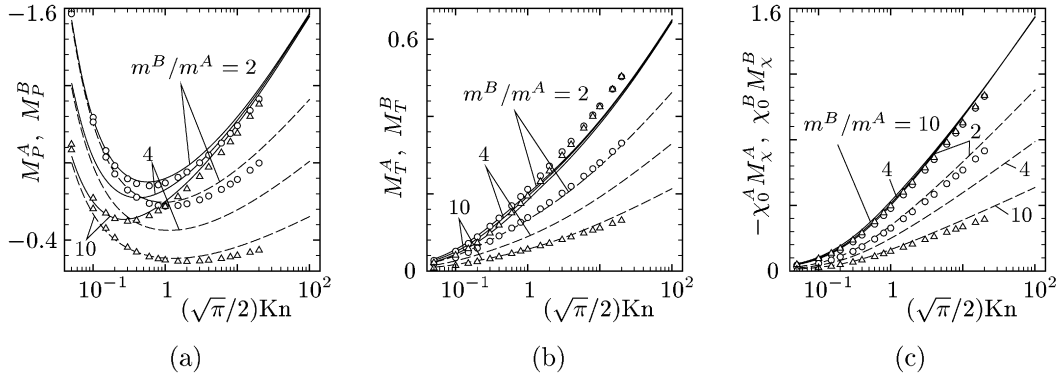

Fig. 1. Particle fluxes M_P^α, M_T^α and M_χ^α vs Kn for virtual gas mixtures composed of hard-sphere molecules in the case of $m^B/m^A = 2$, 4 and 10, $d^B/d^A = 1$ and $\chi_0^A = 0.5$. The —— indicates the results of species A and – – – those of species B. The results of the Boltzmann equation at 18 points of Kn [$0.05 \leqslant (\sqrt{\pi}/2)\mathrm{Kn} \leqslant 20$] obtained in Ref. [19] are also shown by ○ ($m^B/m^A = 2$) and △ ($m^B/m^A = 10$).

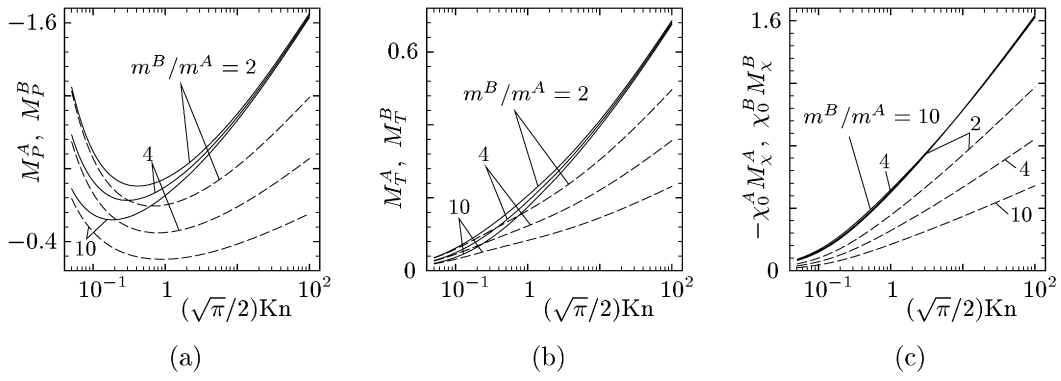

Fig. 2. Particle fluxes M_P^α, M_T^α and M_χ^α vs Kn for virtual gas mixtures composed of the Maxwell molecules in the case of $m^B/m^A = 2$, 4 and 10, $d_*^{BB}/d_*^{AA} = d_*^{BA}/d_*^{AA} = 1$, $\hat{T}_0 = 1$ and $\chi_0^A = 0.5$. See the caption of Fig. 1.

Table 1
Data of molecular interactions between noble gases used in the present work

Species α–β	$d_*^{\beta\alpha} \times 10^8$(cm)				$\nu^{\beta\alpha}$	$\epsilon^{\beta\alpha}/\kappa$(K)
	HS	Maxwell	IPL	LJ	IPL	LJ
He–He	2.193[a]	2.58	2.50	2.70[b]	13.7[c]	6.03[b]
Ne–Ne	2.602[a]	3.06	2.97	2.80[b]	13.4[c]	35.7[b]
Ar–Ar	3.659[a]	4.30	4.32	3.42[b]	7.5[c]	124[b]
He–Ne	2.40[d]	3.00	2.74	2.64[e]	13.55[f]	23.7[e]
He–Ar	2.93[d]	3.50	3.32	2.98[e]	9.6[f]	40.2[e]
Ne–Ar	3.13[d]	3.85	3.66	3.11[e]	9.53[f]	61.7[e]

[a] In the fourth column of Table 11 in Ref. [21], p. 228.
[b] In the second and third column of Table 17 in Ref. [21], p. 237.
[c] In the third column of Table 14 in Ref. [21], p. 232.
[d] In the fifth column of Table 22 in Ref. [21], p. 263. Data by the rule of $d_*^{\beta\alpha} = (d_*^{\beta\beta} + d_*^{\alpha\alpha})/2$.
[e] In the sixth and seventh column of Table 23 in Ref. [21], p. 265.
[f] Data by the rule of $-1 + 2(\nu^{\alpha\alpha}\nu^{\beta\beta} - 1)/(\nu^{\alpha\alpha} + \nu^{\beta\beta} - 2)$. This is often used in the literature when experimental data is not available.

1.30(IPL) and 1.52(LJ)]. It should be noted again that the results of the HS molecule are independent of $\hat{T}_0$, and so those in Figs. 4 and 5 are the same as those in Fig. 3. The analyses for the Maxwell molecule were performed only for $\hat{T}_0 = 1$, since the results at other $\hat{T}_0$ can be obtained by Eq. (4.5). In the case of the IPL and LJ models, we carried

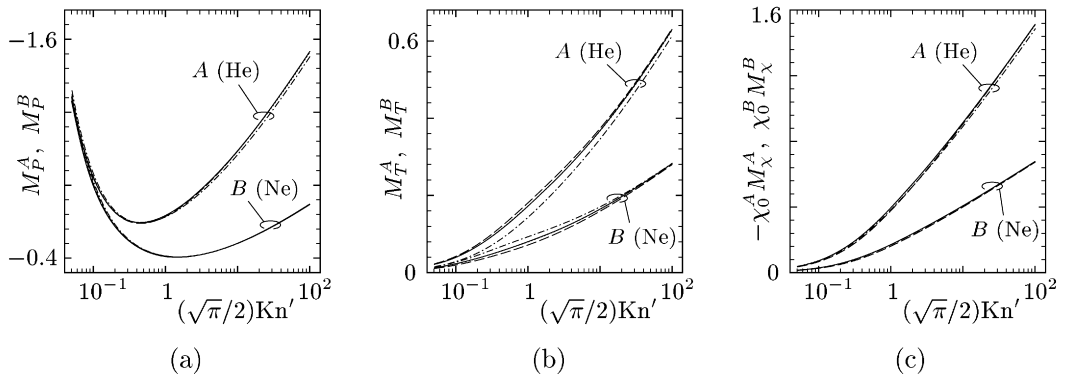

Fig. 3. Particle fluxes M_P^α, M_T^α and M_χ^α vs Kn′ for He (species A) and Ne (species B) in the case of $\chi_0^A = 0.5$ and $\hat{T}_0 = 1$ ($T_0 = 273$ K). The —— indicates the results of the LJ model, ····· those of the IPL model, – – – those of the hard-sphere molecule and — · — those of the Maxwell molecule.

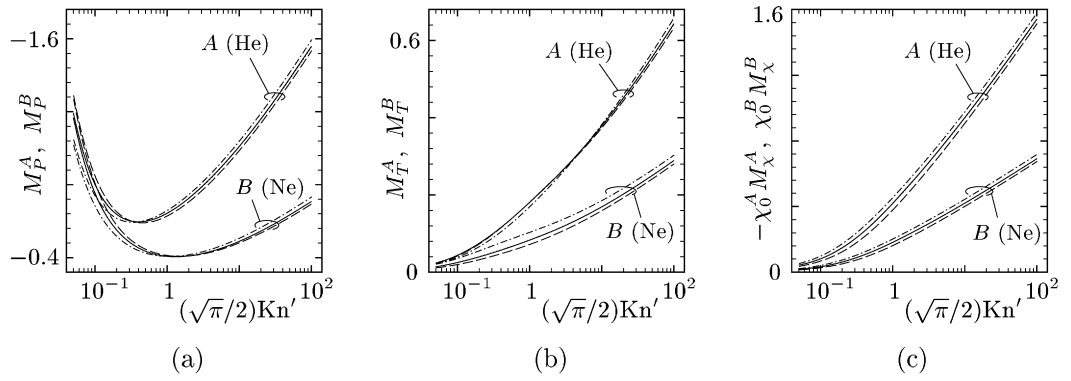

Fig. 4. Particle fluxes M_P^α, M_T^α and M_χ^α vs Kn′ for He (species A) and Ne (species B) in the case of $\chi_0^A = 0.5$ and $\hat{T}_0 = 2$ ($T_0 = 546$ K). See the caption of Fig. 3.

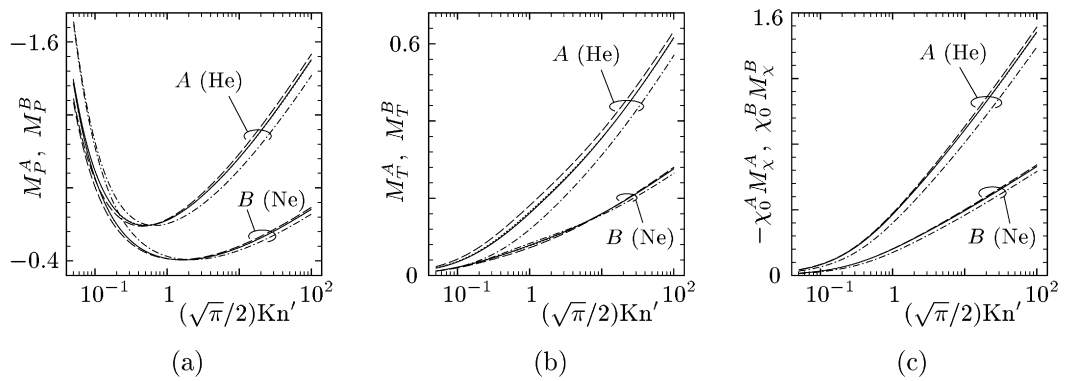

Fig. 5. Particle fluxes M_P^α, M_T^α and M_χ^α vs Kn′ for He (species A) and Ne (species B) in the case of $\chi_0^A = 0.5$ and $\hat{T}_0 = 0.5$ ($T_0 = 136.5$ K). See the caption of Fig. 3.

out the analyses and constructed the databases at five temperatures $\hat{T}_0 = 0.5$, 0.7, 1, 1.5 and 2. In Fig. 3, except for the Maxwell molecule in Fig. 3(b), all the molecular models give almost the same results, since the viscosity and mutual diffusion coefficient (or Ω_{22}^{AA}, Ω_{22}^{BB} and Ω_{11}^{BA}) are almost common at $\hat{T}_0 = 1$. The difference between M_T^A and M_T^B of the Maxwell molecule tends to vanish as Kn′ decreases, as was also seen in Fig. 2 (see the second to last paragraph in Section 4.2). In Figs. 4 and 5, we can see more clearly the difference between the results of respective

molecular models. However, the results of the IPL and LJ models are very close even in these figures and more or less lie between the results of the HS and Maxwell molecule.

We should stress again that the databases constructed and provided as Electronic Annex 2 can reproduce values of M_J^α's in the entire range of Kn and χ_0^A, whereas their behaviour only at $\chi_0^A = 0.5$ in the limited range of Kn is shown in Figs. 3–5. Supplementary figures and more detailed numerical data are presented as Figs. 2 and 3 and Tables 19–45 in Electronic Annex 1 in the online version of this article.

5. Data of computations

In the following three subsections, we briefly summarize the data of computations performed for the construction of the flux database.

5.1. Data of the finite-difference analysis for intermediate Knudsen numbers

We carried out the finite-difference analysis of the boundary-value problem (2.16), (2.21a) and (2.21b) in the range $0.01 \leqslant (\sqrt{\pi}/2)\mathrm{Kn} \leqslant 400$. The above range of Kn was divided further into three or four small intervals and the formula (4.2) was used in the respective small intervals. In total, we carried out the computations for all pairs of (Kn, χ_0^A) made up of 54–56 different values of $(\sqrt{\pi}/2)\mathrm{Kn}$ in $[0.01, 400]$ and 15–21 different values of χ_0^A in $[0, 1]$.

All the computations were performed with common grid system in the (x_2, ζ_2)-space: 401 nonuniform points for x_2 $(0 \leqslant x_2 \leqslant \frac{1}{2})$ with the maximum interval being 3.74×10^{-3} (at $x_2 = 0$) and the minimum 7.81×10^{-9} (at $x_2 = \frac{1}{2}$); 209 nonuniform points for ζ_2 $[|\zeta_2| \leqslant \zeta_{\max} (\equiv 5.62/\sqrt{\hat{m}^\alpha})]$ with the maximum interval being $0.161/\sqrt{\hat{m}^\alpha}$ (at $|\zeta_2| = \zeta_{\max}$) and the minimum $5 \times 10^{-6}/\sqrt{\hat{m}^\alpha}$ (at $\zeta_2 = 0$).

For the estimate of the accuracy of the computations, we introduced the following δ_J $(J = P, T, \chi)$ and d_i $(i = 1, 2, 3)$ defined as

$$\begin{aligned} &\delta_P = \max_{x_2} |P_P + x_2|, \\ &\delta_J = \max_{x_2} |P_J| \quad (J = T, \chi), \end{aligned} \tag{5.1}$$

and

$$\begin{aligned} &d_1 = \big|(\Lambda_{PT} - \Lambda_{TP})/\Lambda_{TP}\big|, \qquad d_2 = \big|(\Lambda_{\chi P} - \Lambda_{P\chi})/\Lambda_{\chi P}\big|, \\ &d_3 = \big|(\Lambda_{T\chi} - \Lambda_{\chi T})/\Lambda_{\chi T}\big|, \end{aligned} \tag{5.2}$$

with

$$\begin{aligned} \Lambda_{PJ} &= 2\int_0^{1/2} (\chi_0^A u_J^A + \chi_0^B u_J^B)\,\mathrm{d}x_2, \\ \Lambda_{TJ} &= 2\int_0^{1/2} (Q_J^A + Q_J^B)\,\mathrm{d}x_2, \\ \Lambda_{\chi J} &= 2\int_0^{1/2} (u_J^A - u_J^B)\,\mathrm{d}x_2 \quad (J = P, T, \chi). \end{aligned} \tag{5.3}$$

Both δ_J's and d_i's are zero theoretically because of Eq. (2.14) for the former and of Onsager's reciprocity relation [35] for the latter. In the actual computations, however, they are not so exactly because of the numerical error, giving a measure of accuracy of the present computations. In all the computations, we have $\delta_J < 1.0 \times 10^{-11}$ and $d_i < 6.4 \times 10^{-5}$ in the case of $0.01 \leqslant (\sqrt{\pi}/2)\mathrm{Kn} \leqslant 0.05$, $\delta_J < 3.8 \times 10^{-13}$ and $d_i < 2.4 \times 10^{-5}$ in the case of $0.05 \leqslant (\sqrt{\pi}/2)\mathrm{Kn} \leqslant 20$ and $\delta_J < 3.4 \times 10^{-14}$ and $d_i < 4.1 \times 10^{-8}$ in the case of $20 \leqslant (\sqrt{\pi}/2)\mathrm{Kn} \leqslant 400$.

5.2. Data of the analysis of the Knudsen-layer problem

As mentioned in the footnote in Section 3.1.2, the Knudsen-layer problem (3.8), (3.9a) and (3.9b) has a unique solution if and only if the slip coefficient $b_{J(n)}$ takes a special value. In principle, the solution can be obtained by repeating the computations with different values of $b_{J(n)}$ until the condition (3.9b) is satisfied. However, since such a repetition is inefficient, we followed the method devised in Ref. [36] (see also Ref. [32]).

We carried out finite-difference analyses of the Knudsen-layer problem for 21 different values of χ_0^A and constructed the formulas for $b_{J(n)}$ and $\mathcal{M}^\alpha_{J(n)}$ similar to Eq. (4.2) using the Chebyshev polynomial approximation. In the computations, we used 651 nonuniform grid points for the space coordinate η [$0 \leqslant \eta \leqslant 47.38$] with the minimum interval being 3.10×10^{-7} (at $\eta = 0$) and the maximum 0.114 (for $13.29 < \eta$). As for the molecular velocity c, we used the same grid points as those for ζ_2 in Section 5.1. As a measure of the accuracy, we have $|S_{J(n)}| < 4.2 \times 10^{-11}$ [see Eq. (3.10)] in all the computations.

5.3. Data of the numerical analysis of the integral equations

We first explain the method of the direct numerical analysis of the integral equations (3.16a)–(3.16c). Let $x_{(i)}$ [$0 = x_{(0)} < x_{(1)} < \cdots < x_{(2N-1)} < x_{(2N)} = \frac{1}{2}$] be the grid points in x_2. The value of a function of x_2 at a grid point $x_{(i)}$ is represented by subscript "(i)", i.e., $u^\alpha_{(i)} = u^\alpha(x_{(i)})$, $L^\alpha_{1(i)} = L^\alpha_1(x_{(i)})$, etc. Here and in the following, we omit the subscript J ($J = P, T, \chi$) which distinguishes the kind of the flow. We first express L^α_n ($n = 1, 2, 3$) in the integrands in Eqs. (3.16a)–(3.16c) using $L^\alpha_{n(i)}$ and sectionally quadratic functions $w^{(j)}_l$ as follows:

$$\begin{aligned} L^\alpha_n(s) &= \sum_{j=0}^{N-1} \sum_{l=0}^{2} L^\alpha_{n(2j+l)} w^{(j)}_l(s), \\ w^{(j)}_l(s) &= \chi_{(j)}(s) \prod_{\substack{k=0 \\ (k\neq l)}}^{2} \frac{s - x_{(2j+k)}}{x_{(2j+l)} - x_{(2j+k)}}, \end{aligned} \tag{5.4}$$

with $\chi_{(j)}$ ($j = 0, 1, \ldots, N-1$) being the characteristic function of the interval $[x_{(2j)}, x_{(2j+2)}]$, i.e., $\chi_{(j)}(s) = 1$ for $x_{(2j)} \leqslant s \leqslant x_{(2j+2)}$ and $\chi_{(j)}(s) = 0$ otherwise. Then, we substitute Eq. (5.4) into Eqs. (3.16a)–(3.16c) and evaluate the resulting expressions at a grid point $x_{(i)}$. As a result, we obtain discretized version of Eqs. (3.16a)–(3.16c). For example, Eq. (3.16a) becomes

$$\begin{aligned} \chi^\alpha_0 u^\alpha_{(i)} = {} & I^\alpha_{U(i)} + \sum_{j=0}^{N-1} \sum_{l=0}^{2} \left[\frac{\mathrm{Kn}}{C^\alpha} \Omega^{\alpha(l)}_{(i,j)}[\Delta_G] \left(L^\alpha_{1(2j+l)} - \frac{1}{2} L^\alpha_{3(2j+l)} \right) \right. \\ & \left. - \Omega^{\alpha(l)}_{(i,j)}[\Delta_0''] L^\alpha_{2(2j+l)} + \sqrt{\hat{m}^\alpha} \Omega^{\alpha(l)}_{(i,j)}[\Delta_1] L^\alpha_{3(2j+l)} \right]. \end{aligned} \tag{5.5}$$

The $\Omega^{\alpha(l)}_{(i,j)}$ is the numerical integral kernel and is defined as

$$\Omega^{\alpha(l)}_{(i,j)}[h] = \frac{1}{\mathrm{Kn}} \int_{x_{(2j)}}^{x_{(2j+2)}} w^{(j)}_l(s) h\left(s + x_{(i)}, s - x_{(i)}; \frac{\tilde{C}^\alpha}{\mathrm{Kn}} \right) \mathrm{d}s, \tag{5.6}$$

where h represents Δ_G, Δ_1, etc. Note that the numerical integral kernel does not depend on the subscript J, that is, it is common to all the flows.

We carried out numerical analyses of the discretized integral equations in the range $100 \leqslant (\sqrt{\pi}/2)\mathrm{Kn} \leqslant 10^4$ and $10^4 \leqslant (\sqrt{\pi}/2)\mathrm{Kn} \leqslant 10^6$ separately, and used the formula (4.2) with $N_\mathrm{K} = N_\chi = 8$ in each range. We used 201 uniform grid points in x_2 ($0 \leqslant x_2 \leqslant \frac{1}{2}$) in the former range and 101 uniform grid points in the latter. The integral kernels $\Omega^{\alpha(l)}_{(i,j)}$ were prepared by applying the Gauss–Legendre formula to Eq. (5.6). As a measure of the accuracy, we have $\delta_J < 5.0 \times 10^{-8}$ and $d_i < 2.7 \times 10^{-7}$ in all the computations in the former range of Kn and $\delta_J < 2.8 \times 10^{-10}$ and $d_i < 4.7 \times 10^{-9}$ in those in the latter.

6. Conclusions

The elemental channel flows, i.e., the Poiseuille flow, thermal transpiration and concentration-driven flow of binary gas mixtures between two parallel plates, were investigated on the basis of the McCormack model equation and the diffuse reflection boundary condition. We first analyzed the problem numerically by means of a finite-difference method for intermediate Knudsen numbers. Then we carried out the asymptotic analysis for small Knudsen numbers and the finite-difference analysis of the associated Knudsen-layer problems. For large Knudsen numbers, the system of integral equations for macroscopic quantities was derived and was analyzed numerically and analytically.

The analyses were performed in the case of virtual gas mixtures composed of hard-sphere molecules or the Maxwell molecules and in the case of mixtures of noble gases (He–Ne, He–Ar and Ne–Ar). In the former case, the results for hard-sphere molecules were compared with corresponding results of the Boltzmann equation. In the latter case, the inverse power-law potential and Lennard-Jones 12,6 models, as well as the hard-sphere and Maxwell molecule, were employed, and their results were compared one another.

Making use of the above results, we constructed the database of the particle flux covering the entire ranges of the Knudsen number and of the concentration and a wide range of the temperature. The database constructed and provided as Electronic Annex 2 in the online version of this article can be incorporated in the generalized Reynolds equation as well as the fluid-dynamic model in Ref. [3] describing the behaviour of a binary gas mixture in the Knudsen compressor.

Acknowledgements

S. K. thanks Professor Pierre Degond for his hospitality during the stay in Toulouse, which is supported by the grant from the Kyoto University Foundation. Part of the computations were performed on SGI Origin 3800 in the Supercomputer Laboratory, Institute for Chemical Research, Kyoto University.

Appendix A. Macroscopic quantities

The macroscopic quantities ω^α, u_i^α, etc. of species α are defined in terms of moments of ϕ^α as follows:

$$\begin{aligned}
&\omega^\alpha = \int \phi^\alpha E^\alpha \,\mathrm{d}^3\boldsymbol{\zeta}, \qquad u_i^\alpha = \frac{1}{\chi_0^\alpha}\int \zeta_i \phi^\alpha E^\alpha \,\mathrm{d}^3\boldsymbol{\zeta},\\
&P^\alpha = \omega^\alpha + \chi_0^\alpha \theta^\alpha = \frac{2}{3}\hat{m}^\alpha \int |\boldsymbol{\zeta}|^2 \phi^\alpha E^\alpha \,\mathrm{d}^3\boldsymbol{\zeta},\\
&P_{ij}^\alpha = 2\hat{m}^\alpha \int \zeta_i \zeta_j \phi^\alpha E^\alpha \,\mathrm{d}^3\boldsymbol{\zeta},\\
&Q_i^\alpha = \int \zeta_i \left(\hat{m}^\alpha |\boldsymbol{\zeta}|^2 - \frac{5}{2}\right)\phi^\alpha E^\alpha \,\mathrm{d}^3\boldsymbol{\zeta},
\end{aligned} \tag{A.1}$$

with $\mathrm{d}^3\boldsymbol{\zeta} = \mathrm{d}\zeta_1\,\mathrm{d}\zeta_2\,\mathrm{d}\zeta_3$. The integrations are performed over the whole space of $\boldsymbol{\zeta}$. The macroscopic quantities of the mixture are expressed in terms of those of the component species as

$$\begin{aligned}
&\omega = \sum_{\beta=A,B} \omega^\beta, \qquad u_i = \left(\sum_{\beta=A,B} \hat{m}^\beta \chi_0^\beta u_i^\beta\right)\left(\sum_{\beta=A,B} \hat{m}^\beta \chi_0^\beta\right)^{-1},\\
&P = \omega + \theta = \sum_{\beta=A,B} P^\beta, \qquad P_{ij} = \sum_{\beta=A,B} P_{ij}^\beta,\\
&Q_i = \sum_{\beta=A,B}\left[Q_i^\beta - \frac{5}{2}\chi_0^\beta (u_i - u_i^\beta)\right].
\end{aligned} \tag{A.2}$$

Appendix B. Chapman–Cowling integral

We shall show below the nondimensional counterpart $\hat{\Omega}_{ij}^{\beta\alpha}$ of the Chapman–Cowling integral $\Omega_{ij}^{\beta\alpha}$ for several molecular models used in the present work. The $\hat{\Omega}_{ij}^{\beta\alpha}$ is defined as

$$\hat{\Omega}_{ij}^{\beta\alpha} = \frac{1}{\pi (d_*^{\beta\alpha})^2}\left[\frac{m^\beta m^\alpha}{2\kappa T_0 (m^\beta + m^\alpha)}\right]^{1/2} \Omega_{ij}^{\beta\alpha}(T_0). \tag{B.1}$$

B.1. Hard-sphere molecule

The reference diameter $d_*^{\beta\alpha}$ in β–α collisions is defined as $d_*^{\beta\alpha} = (d^\beta + d^\alpha)/2$ with d^α being the molecular diameter of species α. The $\Omega_{ij}^{\beta\alpha}$ for this molecular model is given by Eqs. (10.1,1) and (10.2,1) in Ref. [21]. Following the definition (B.1), we have

$$\hat{\Omega}_{ij}^{\beta\alpha} = \frac{1}{8\sqrt{\pi}}\left[2 - \frac{1 + (-1)^i}{i+1}\right](j+1)!. \tag{B.2}$$

Note that $\hat{\Omega}_{ij}^{\beta\alpha}$ in this case is independent of $\hat{T}_0$.

B.2. Inverse power-law potential model

In this model, the potential $U^{\beta\alpha}$ of intermolecular force between species β and α is given by $U^{\beta\alpha}(r) = a^{\beta\alpha}/r^{\nu^{\beta\alpha}-1}$ with r being the distance between the centre of the molecules and $a^{\beta\alpha}$ and $\nu^{\beta\alpha}(\geqslant 3)$ the positive constants. The $\Omega_{ij}^{\beta\alpha}$ for this model is given by Eq. (10.31,7) in Ref. [21]. The definition of $d_*^{\beta\alpha}$ and expression of $\hat{\Omega}_{ij}^{\beta\alpha}$ are as follows:

$$\begin{aligned}
\hat{\Omega}_{ij}^{\beta\alpha} &= \frac{1}{2\sqrt{\pi}} \hat{T}_0^{\frac{-2}{\nu^{\beta\alpha}-1}} A_i(\nu^{\beta\alpha}) \Gamma\left(j + 2 - \frac{2}{\nu^{\beta\alpha}-1}\right), \\
d_*^{\beta\alpha} &= \left(\frac{(\nu^{\beta\alpha}-1)a^{\beta\alpha}}{2\kappa T_*}\right)^{\frac{1}{\nu^{\beta\alpha}-1}},
\end{aligned} \tag{B.3}$$

where $\hat{T}_0 = T_0/T_*$, Γ the gamma function and A_i a function of $\nu^{\beta\alpha}$ defined by Eq. (10.31,6) in Ref. [21]. The $\hat{\Omega}_{ij}^{\beta\alpha}$ in this case depends on $\hat{T}_0$.

The Maxwell molecular model is a special kind of the inverse power-law potential model whose exponents are commonly set as $\nu^{\beta\alpha} = 5$. It is seen from Eq. (B.3) that $\hat{\Omega}_{ij}^{\beta\alpha}$'s in this case are commonly proportional to $\hat{T}_0^{-1/2}$. Since this common factor can be included in Kn [see Eqs. (2.8)–(2.12) and (C.3) in Appendix C], one obtains Eq. (4.5) in the case of the Maxwell molecules.

B.3. Lennard-Jones 12,6 model

In this model, the potential $U^{\beta\alpha}$ of intermolecular force between species β and α is given by $U^{\beta\alpha}(r) = 4\epsilon^{\beta\alpha}[(d_*^{\beta\alpha}/r)^{12} - (d_*^{\beta\alpha}/r)^6]$ with r being the distance between the centre of the molecules and $\epsilon^{\beta\alpha}$ the positive constant [i.e., $d_*^{\beta\alpha}$ is defined so that $U^{\beta\alpha}(d_*^{\beta\alpha}) = 0$]. The $\hat{\Omega}_{ij}^{\beta\alpha}$ for this model is a function of $\hat{T}_0$. Since its functional form can not be obtained analytically, we constructed that only numerically.

Appendix C. Transport coefficients

The Chapman–Enskog method [21] or Sone's asymptotic theory [24,25,9] (see also Ref. [26]) leads to the following expressions of the transport coefficients for the McCormack model equation. The viscosity μ, thermal conductivity λ, mutual diffusion coefficient D_{AB} and thermal diffusion coefficient D_T are expressed as

$$\begin{aligned}
&\mu = \hat{\mu}\left(\frac{m^A}{2\kappa T_0}\right)^{1/2} p_0 l_0, \qquad \lambda = \hat{\lambda}\frac{2\kappa}{m^A}\left(\frac{m^A}{2\kappa T_0}\right)^{1/2} p_0 l_0,\\
&D_{AB} = \hat{D}_{AB}\left(\frac{2\kappa T_0}{m^A}\right)^{1/2} l_0, \qquad D_T = \hat{D}_T\left(\frac{2\kappa T_0}{m^A}\right)^{1/2} l_0,
\end{aligned} \tag{C.1}$$

with

$$\begin{aligned}
&\hat{\mu} = \hat{\mu}^A + \hat{\mu}^B, \qquad \hat{\lambda} = \hat{\lambda}^A + \hat{\lambda}^B,\\
&\hat{D}_{AB} = \frac{1}{2\nu_{BA}^{(1)} K^{BA}}\left[1 - \left(\frac{\hat{D}^B}{\hat{m}^B \chi_0^B} + \frac{\hat{D}^A}{\chi_0^A}\right)\frac{\nu_{BA}^{(2)}}{\nu_{BA}^{(1)}}\right]^{-1},\\
&\hat{D}_T = 2\chi_0^B \chi_0^A \nu_{BA}^{(2)} K^{BA}\left(\frac{\hat{\lambda}^B}{\hat{m}^B \chi_0^B} - \frac{\hat{\lambda}^A}{\chi_0^A}\right)\hat{D}_{AB} = (\hat{D}^B - \hat{D}^A)\hat{D}_{AB},
\end{aligned} \tag{C.2}$$

and

$$\begin{aligned}
&\hat{\mu}^\alpha = \chi_0^\alpha \frac{\Psi^\beta + \chi_0^\beta \nu_{\beta\alpha}^{(4)} K^{\beta\alpha}}{\Psi^\alpha \Psi^\beta - \chi_0^\alpha \chi_0^\beta \nu_{\alpha\beta}^{(4)} \nu_{\beta\alpha}^{(4)} (K^{\beta\alpha})^2},\\
&\hat{\lambda}^\alpha = \frac{5}{4}\chi_0^\alpha \frac{(\Gamma^\beta/\hat{m}^\alpha) + (\chi_0^\beta \nu_{\beta\alpha}^{(6)} K^{\beta\alpha}/\hat{m}^\beta)}{\Gamma^\alpha \Gamma^\beta - \chi_0^\alpha \chi_0^\beta \nu_{\alpha\beta}^{(6)} \nu_{\beta\alpha}^{(6)} (K^{\beta\alpha})^2},\\
&\hat{D}^\alpha = \frac{5}{2}\chi_0^\beta \chi_0^\alpha K^{\beta\alpha} \frac{(\nu_{\beta\alpha}^{(2)} \Gamma^\beta/\hat{m}^\alpha) - (\chi_0^\alpha \nu_{\alpha\beta}^{(2)} \nu_{\beta\alpha}^{(6)} K^{\beta\alpha}/\hat{m}^\beta)}{\Gamma^\alpha \Gamma^\beta - \chi_0^\alpha \chi_0^\beta \nu_{\alpha\beta}^{(6)} \nu_{\beta\alpha}^{(6)} (K^{\beta\alpha})^2},\\
&\Psi^\alpha = \chi_0^\alpha (\nu_{\alpha\alpha}^{(3)} - \nu_{\alpha\alpha}^{(4)}) K^{\alpha\alpha} + \chi_0^\beta \nu_{\beta\alpha}^{(3)} K^{\beta\alpha},\\
&\Gamma^\alpha = \chi_0^\alpha (\nu_{\alpha\alpha}^{(5)} - \nu_{\alpha\alpha}^{(6)}) K^{\alpha\alpha} + \chi_0^\beta \nu_{\beta\alpha}^{(5)} K^{\beta\alpha}.
\end{aligned} \tag{C.3}$$

Suppose that $\beta \neq \alpha$ in Eq. (C.3), i.e., $\beta = B$ for $\alpha = A$ and $\beta = A$ for $\alpha = B$. The μ, λ, D_{AB} and thermo–diffusion ratio $k_T (= D_T/D_{AB})$ for the McCormack model coincide with the corresponding results for the Boltzmann equation obtained by the Chapman–Enskog method at the first or second approximation. To be more specific, μ, λ, k_T and D_{AB} here coincide, respectively, with $[\mu]_1$, $[\lambda]_1$, $[k_T]_1$ (the first approximation) and $[D_{12}]_2$ (the second approximation) in Ref. [21].

Supplementary material

The online version of this article contains additional supplementary material.
Please visit DOI: 10.1016/j.euromechflu.2007.08.002.

References

[1] S. Fukui, R. Kaneko, Analysis of ultra-thin gas film lubrication based on linearized Boltzmann equation including thermal creep flow, J. Tribol. 110 (1988) 253–262.
[2] C. Shen, Use of the degenerated Reynolds equation in solving the microchannel flow problem, Phys. Fluids 17 (2005) 046101.
[3] S. Takata, H. Sugimoto, S. Kosuge, Gas separation by means of the Knudsen compressor, Eur. J. Mech. B/Fluids 26 (2007) 155–181.
[4] M. Knudsen, Eine Revision Gleichgewichtsbedingung der Gase. Thermische Molekularströmung, Ann. Phys. (Leipzig) 31 (1910) 205–229.
[5] G. Pham-Van-Diep, P. Keeley, E.P. Muntz, D.P. Weaver, A micromechanical Knudsen compressor, in: J. Harvey, G. Lord (Eds.), Rarefied Gas Dynamics, vol. I, Oxford University Press, London, 1995, pp. 715–721.
[6] Y. Sone, Y. Waniguchi, K. Aoki, One-way flow of a rarefied gas induced in a channel with a periodic temperature distribution, Phys. Fluids 8 (1996) 2227–2235.
[7] C. Cercignani, M. Lampis, S. Lorenzani, Plane Poiseuille–Couette problem in micro-electro-mechanical systems applications with gas-rarefaction effects, Phys. Fluids 18 (2006) 087102.
[8] J.C. Maxwell, On stresses in rarefied gases arising from inequalities of temperature, Philos. Trans. Roy. Soc. 170 (1879) 231–256.
[9] Y. Sone, Kinetic Theory and Fluid Dynamics, Birkhäuser, Boston, 2002.

[10] T. Ohwada, Y. Sone, K. Aoki, Numerical analysis of the Poiseuille and thermal transpiration flows between two parallel plates on the basis of the Boltzmann equation for hard-sphere molecules, Phys. Fluids A 1 (1989) 2042–2049; Erratum: Phys. Fluids A 2 (1990) 639.
[11] F. Sharipov, V. Seleznev, Data on internal rarefied gas flows, J. Phys. Chem. Ref. Data 27 (1998) 657–706.
[12] V.G. Chernyak, V.V. Kalinin, P.E. Suetin, The kinetic phenomena in nonisothermal motion of a binary gas through a plane channel, Int. J. Heat Mass Transfer 27 (1984) 1189–1196.
[13] Y. Onishi, On the behaviour of a slightly rarefied gas mixture over plane boundaries, Z. Angew. Math. Phys. 37 (1986) 573–596.
[14] C.M. Huang, R.V. Tompson, T.K. Ghosh, I.N. Ivchenko, S.K. Loyalka, Measurements of thermal creep in binary gas mixtures, Phys. Fluids 11 (1999) 1662–1672.
[15] F. Sharipov, D. Kalempa, Gaseous mixture flow through a long tube at arbitrary Knudsen numbers, J. Vac. Sci. Technol. A 20 (2002) 814–822.
[16] S. Naris, D. Valougeorgis, D. Kalempa, F. Sharipov, Gaseous mixture flow between two parallel plates in the whole range of the gas rarefaction, Physica A 336 (2004) 294–318.
[17] C.E. Siewert, D. Valougeorgis, The McCormack model: channel flow of a binary gas mixture driven by temperature, pressure and density gradients, Eur. J. Mech. B/Fluids 23 (2004) 645–664.
[18] S. Naris, D. Valougeorgis, D. Kalempa, F. Sharipov, Flow of gaseous mixtures through rectangular microchannels driven by pressure, temperature, and concentration gradients, Phys. Fluids 17 (2005) 100607.
[19] S. Kosuge, K. Sato, S. Takata, K. Aoki, Flows of a binary mixture of rarefied gases between two parallel plates, in: M. Capitelli (Ed.), Rarefied Gas Dynamics, AIP, New York, 2005, pp. 150–155.
[20] F.J. McCormack, Construction of linearized kinetic models for gaseous mixtures and molecular gases, Phys. Fluids 16 (1973) 2095–2105.
[21] S. Chapman, T.G. Cowling, The Mathematical Theory of Non-Uniform Gases, third ed., Cambridge University Press, Cambridge, 1990.
[22] C. Cercignani, F. Sharipov, Gaseous mixture slit flow at intermediate Knudsen numbers, Phys. Fluids A 4 (1992) 1283–1289.
[23] C.K. Chu, Kinetic-theoretic description of the formation of a shock wave, Phys. Fluids 8 (1965) 12–22.
[24] Y. Sone, Asymptotic theory of flow of rarefied gas over a smooth boundary I, in: L. Trilling, H.Y. Wachman (Eds.), Rarefied Gas Dynamics, vol. I, Academic Press, New York, 1969, pp. 243–253.
[25] Y. Sone, Asymptotic theory of flow of rarefied gas over a smooth boundary II, in: D. Dini (Ed.), Rarefied Gas Dynamics, vol. II, Editrice Tecnico Scientifica, Pisa, 1971, pp. 737–749.
[26] S. Takata, K. Aoki, The ghost effect in the continuum limit for a vapor–gas mixture around condensed phases: Asymptotic analysis of the Boltzmann equation, Transp. Theory Stat. Phys. 30 (2001) 205–237; Erratum: Transp. Theory Stat. Phys. 31 (2002) 289.
[27] K. Aoki, C. Bardos, S. Takata, Knudsen layer for gas mixtures, J. Stat. Phys. 112 (2003) 629–655.
[28] C. Cercignani, Plane Poiseuille flow and Knudsen minimum effect, in: J.A. Laurmann (Ed.), Rarefied Gas Dynamics, vol. II, Academic Press, New York, 1963, pp. 92–101.
[29] C. Cercignani, Plane Poiseuille flow according to the method of elementary solutions, J. Math. Anal. Appl. 12 (1965) 254–262.
[30] H. Niimi, Thermal creep flow of rarefied gas between two parallel plates, J. Phys. Soc. Jpn. 30 (1971) 572–574.
[31] M. Abramowitz, I.A. Stegun, Handbook of Mathematical Functions, Dover, New York, 1968.
[32] S. Takata, S. Yasuda, S. Kosuge, K. Aoki, Numerical analysis of thermal-slip and diffusion-slip flows of a binary mixture of hard-sphere molecular gases, Phys. Fluids 15 (2003) 3745–3766.
[33] C. Gasquet, P. Witomski, Fourier Analysis and Applications, Springer-Verlag, New York, 1999.
[34] C. Cercignani, The Boltzmann Equation and Its Applications, Springer-Verlag, New York, 1988.
[35] F. Sharipov, Onsager–Casimir reciprocity relations for open gaseous systems at arbitrary rarefaction. III. Theory and its application for gaseous mixtures, Physica A 209 (1994) 457–476.
[36] T. Ohwada, Y. Sone, K. Aoki, Numerical analysis of the shear and thermal creep flows of a rarefied gas over a plane wall on the basis of the linearized Boltzmann equation for hard-sphere molecules, Phys. Fluids A 1 (1989) 1588–1599.